Wide-Angle Beam Scanning Phased Array Antennas: A Review

MING LI[1], SHU-LIN CHEN[1] (Member, IEEE), YANHUI LIU[2] (Senior Member, IEEE), AND Y. JAY GUO[1] (Fellow, IEEE)

[1]Global Big Data Technologies Centre (GBDTC), University of Technology Sydney, NSW 2007 , Australia.
[2]School of Electronic Science and Engineering, University of Electronic Science and Technology of China, Sichuan 610054, China

CORRESPONDING AUTHOR: SHU-LIN CHEN

ABSTRACT Phased array antennas (PAAs) with flexible and agile wide-angle beam scanning (WABS) abilities have drawn rapidly increasing attentions in recent years. They have found significant applications in beyond fifth-generation (B5G) and sixth-generation (6G) wireless communications, satellite communications, sensing, etc., for their outstanding capability to achieve wide spatial coverage, enable critical frequency reuse, and improve the system capacity. In this review, we aim to investigate and discuss several challenges that hinder WABS for conventional PAAs, including the strong mutual coupling, narrow beamwidth of the element antenna, etc. We then review and summarize a variety of innovative techniques to overcome these challenges. Subsequently, we discuss and analyze potential research gaps of WABS PAAs for future emerging applications. This timely review fulfills the demand of a thorough and detailed investigation on WABS technologies for PAAs and provides detailed introduction and guidance for interested researchers and engineers.

INDEX TERMS Beyond fifth-generation (B5G), grating lobe, mutual coupling, phased array antenna (PAA), sixth-generation (6G), wide-angle beam scanning (WABS), wide-angle impedance matching (WAIM).

I. INTRODUCTION

PHASED array antennas (PAAs), comprising of two or more antenna elements fed coherently with controllable phase shifters to achieve desired pattern performance such as beam scanning and shaping, is a crucial technology for modern communications and sensing systems. The PAA behaves like a choir for a music concert. Each member in the choir, i.e., the antenna element in the PAA, should be well coordinated to produce an insistent high-performance rhythm. PAAs have numerous advantages, and they are capable of achieving high gain, low sidelobe level (SLL), flexible beam scanning, and high tracking accuracy.

Particularly, PAAs capable of agile beam scanning within a wide angular range is a critical enabler for current and future terrestrial and non-terrestrial wireless communications networks [1], [2]. Wide-angle beam scanning (WABS) PAAs can find many significant applications; some of them are shown in Fig. 1. Modern wireless communications have become an ubiquitous part of our daily lives and activities, which results in ever-increasing data traffic and device connections [3]. The data traffic in wireless networks is expected to grow even faster. The beyond fifth-generation (B5G) and sixth-generation (6G) communications are promised to meet the demands in the foreseeable future. They can realize data rates at a level of gigabit per second (Gbps), and bring millisecond-level of latency time, far higher traffic volume density, super dense connections, and improved efficiencies in terms of energy and cost [4]. WABS antennas can deliver critical frequency reuse and significantly improved system capacity, which has been considered as a key enabler technology for B5G and 6G communications [5]–[8].

Over the past decade, we have also witnessed an increasing demand for satellite communications (SATCOMs) [9]. Some commercial companies like Starlink, OneWeb, and Kuiper have already begun their race of launching space-based broadband communication satellites. In SATCOM, electronic beam steering PAAs are highly desired since they generally have lower profiles than lens or reflector antennas and do not occupy large space as the mechanical scanned arrays. Moreover, with the development of the silicon technology in the past decade, silicon beamformer chips have been employed in large-scale PAAs for SATCOM to reduce the cost and to offer a high degree of integration [9]–[11]. Thus, highly integrated PAAs with WABS ability that can achieve global coverage are becoming very promising in
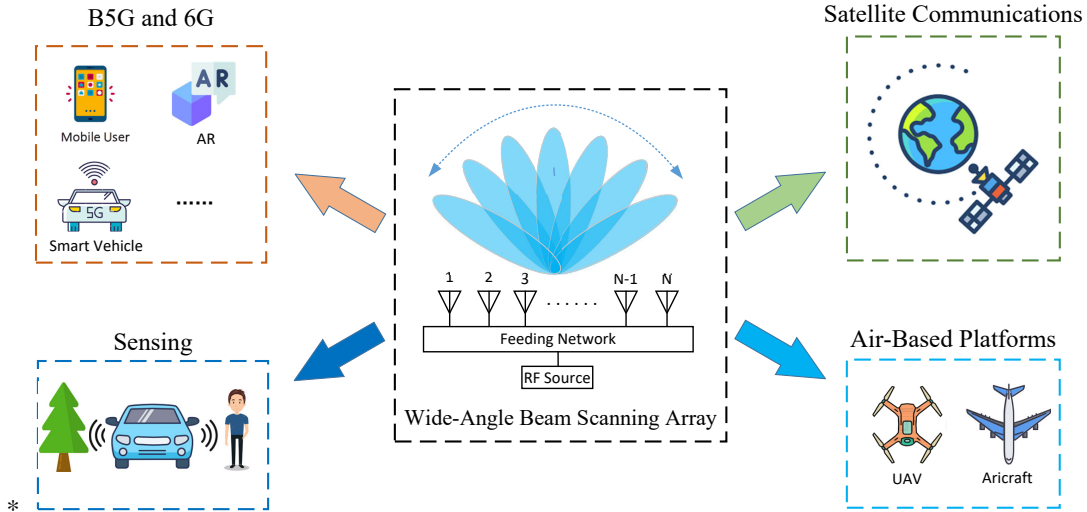
FIGURE 1. Several application scenarios of wide-angle beam scanning (WABS) phased array antennas (PAAs).

SATCOM, especially for medium earth orbit (MEO) and low earth orbit (LEO) SATCOM.

Another important application of WABS PAAs is the sensing-based automotive radar and anti-collision radar. Automotive radar is like the eye of the automobiles; it is a key technology to achieve autonomous driving. It can make driving safer and more convenient by relieving the drivers from monotonic tasks and split-second decisions within complex traffic conditions. WABS PAAs are highly promising candidates given their high-gain scanning beams in a very wide angular range [12], [13]. Furthermore, WABS PAAs can also find applications in airborne platforms like unmanned aerial vehicles (UAVs) [14] and aircrafts [15], synthetic aperture radar [16], etc. This wide range of applications has largely driven the evolution and development of WABS PAA technologies.

The focus of this work is to review and summarize main challenges and recent advances for facilitating WABS with PAAs. Although some literatures have been reported to achieve this objective, there are still some limitations and potential gaps. In [17], Kavitha *et al.* briefly introduced the wide-angle scanning PAAs and reviewed several types of antenna elements suitable for WABS. But the challenges to achieve WABS were not thoroughly discussed, and only a few technologies were discussed. In [18], Li *et al.* briefly discussed the main challenges of achieving WABS and presented a review of wideband WABS. However, they focused on only wideband WABS PAAs with target applications of SATCOM. Besides, it is worth mentioning that a special issue on the low-cost WABS antennas was published recently in [19]. In this special issue, a variety of technologies were developed and reported to achieve low-cost technologies in the theory, design, development, measurements, and in-field deployment of the WABS PAAs. Based on the above state-of-the-art, we present a comprehensive and timely review on WABS PAAs in this paper. We will mainly discuss the challenges and technologies to achieve WABS for linear and planar PAAs. Conformal PAAs, such as cylindrical PAAs that can achieve very wide scanning thanks to their curved structures, are out of the scope of this review. The main contributions of this work are summarized as follows. Firstly, we have comprehensively discussed the main problems and challenges encountered in achieving WABS for linear and planar arrays. In addition, we thoroughly reviewed innovative techniques and strategies to tackle these challenges by category according to their main contributions. Moreover, future research potential gaps are adequately discussed in this paper. It is expected that this paper will facilitate the research, development and technology uptake of WABS arrays in current and future communications and sensing systems.

This paper is organized as follows. In Section II, the background of PAAs is briefly discussed. Section III presents the main challenges in facilitating WABS. In Sections IV, V, VI, and VII, the state-of-the-art achieving WABS by utilizing different technologies are thoroughly reviewed. Section VIII describes the future research potential gaps. Section IX draws the conclusion.

II. BRIEF INTRODUCTION TO PHASED ARRAY ANTENNAS

In this section, the PAA is briefly introduced. Then some popular optimization strategies for designing PAAs to achieve desired radiation performances are summarized.

A. PHASED ARRAY ANTENNAS

PAAs are those that can achieve desired beam pattern performance by individually controlling phase shifters connected to each array element with or without excitation amplitude modulation. PAA scanning is a modern beam scanning technology that evolves from conventional mechanical scanning arrays. It is known that the mechanical scanning arrays have
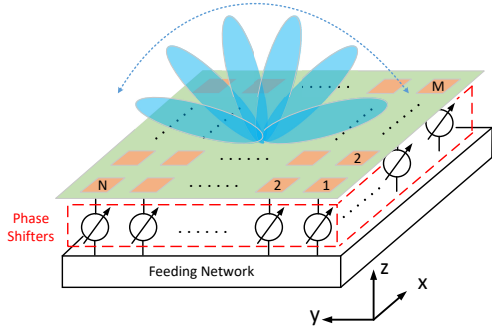
FIGURE 2. Schematic view of a typical planar phased array antenna (PAA) with phase shifters for beam scanning.

to mechanically rotate antenna arrays to steer their main beams. As a consequence, they suffer from many severe issues that hinders their applications for modern wireless systems, such as having a low scanning speed, being bulky and lack of accuracy, etc. On the contrary, benefiting from the use of controllable phase shifters, PAAs usually have a fast scanning speed and high accuracy, and exhibit a high reliability and flexibility in beam steering and shaping.

Fig. 2 shows a schematic view of a typical PAA with a planar array arrangement. As noted, this planar PAA has a total of $M \times N$ individual elements distributed in the xoy-plane. Each element in the array is connected with a phase shifter that provides the requisite phase for beam steering. With the array setup as shown in Fig. 2, the far-field pattern $F(\theta, \phi)$ of this PAA can be expressed as:

$$F(\theta, \phi) = \sum_{m=1}^{M} \sum_{n=1}^{N} I_{m,n} E_{m,n}(\theta, \phi) e^{j\{k_0 \vec{r}_{m,n} \cdot \vec{u}(\theta,\phi) + \alpha_{m,n}\}}$$

(1)

where $j = \sqrt{-1}$; $k_0 = 2\pi/\lambda$ is the wavenumber in free space; θ is the angle measured from positive z-axis and ϕ is the azimuth angle measured from positive x-axis; $E_{m,n}(\theta, \phi)$ denotes the pattern of the element in the mth ($m = 1, 2, ..., M$) row and nth ($n = 1, 2, ..., N$) column; $\vec{u}(\theta, \phi) = \sin\theta\cos\phi\vec{e}_x + \sin\theta\sin\phi\vec{e}_y + \cos\theta\vec{e}_z$ is the propagation direction vector. $\vec{r}_{m,n}$, $I_{m,n}$, and $\alpha_{m,n}$ are the location, excitation amplitude, and excitation phase of the (m, n)th element, respectively. It is common knowledge that one generally can control the excitation phases $\alpha_{m,n}$ and amplitudes $I_{m,n}$ to achieve desired pattern performance of PAAs.

B. OPTIMIZATION STRATEGIES

Generally, besides the intuitive beam scanning, PAAs should be equipped with additional performance optimization for practical applications, such as having low sidelobe levels (SLLs), achieving low cross-polarization levels, suppressing grating lobes, etc. To accomplish the above goals along with the beam scanning, one can optimize the array parameters associated with the PAAs, including the excitation amplitudes and phases, and element positions.

Optimizing both excitation amplitude and phase is a common approach as reported in the literature. Numerous excitation amplitude and phase optimization methods have been developed in the past decades, including the iterative Fourier transform (IFT) and its variants [20]–[22], convex optimization techniques [23], [24], alternating projection methods [25], [26], stochastic algorithms [27], [28], and machine learning methods [29]–[31]. They have achieved scanned beams with excellent performance in terms of main-lobe shape, SLL reduction, and null notching in specified directions.

The phase-only optimization method is another effective approach for PAA pattern synthesis. It avoids using nonuniform excitation amplitudes, thus leading to simplified feeding networks since amplitude weighting requires unequal power dividers. A lot of effective methods were developed in the past to design PAAs employing phase-only optimization [32]–[35]. For example, in [34], an adaptive bat algorithm was developed to achieve pattern nulling at directions of interferences by optimizing the excitation phases only. It was shown that nulls can be precisely imposed to an arbitrary interference direction using the developed bat algorithm-based beamformer.

Over this decade, element rotation was included as a brand new degree of freedom to replace amplitude weighting in the PAA synthesis [36]–[44]. In comparison to conventional amplitude weighting, the method of using element rotation can greatly simplify the feeding network and the associated cost and complexity for the PAAs by saving many unequal power dividers [42]. With the element rotation, beam scanning patterns can be achieved with reduced SLLs [37], [38]. Besides, axial ratio for the circular polarization pattern can be improved with the element rotation technique [39], [40]. Moreover, shaped beam patterns with scanning can also be realized with the developed methods in [42]–[44].

III. CHALLENGES FOR WIDE-ANGLE BEAM SCANNING (WABS)

Achieving WABS for PAAs has been one of the most challenging tasks. Specifically, good impedance matching and consistent gains should be maintained when the beam is scanned in a wide angular range. The wide angular range of PAAs is usually interpreted as being larger than 100°. In the realization of WABS PAAs, there are three key issues to be considered as follows:

The first is the beamwidth of antenna element pattern. Theoretically, gain pattern of an array is the product of the array factor and the element pattern when each element is assumed to have identical radiation pattern [45]. Therefore, for an antenna element with a traditional broadside radiation pattern, the array peak gain will decrease as the beam scans away from broadside due to the gain drop of the element pattern [46]. As an example, a 12-element linear array with uniform inter-element spacing of half wavelength is considered. Its element pattern is assumed to be $\cos\theta$.
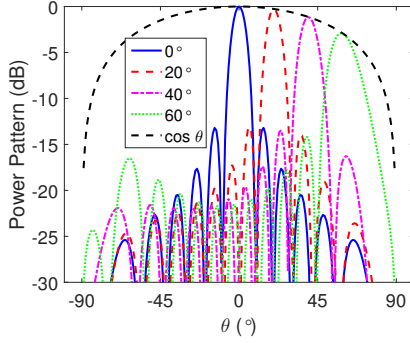
FIGURE 3. Beam scanning patterns for a 12-element linear array with the element pattern of $\cos\theta$.

Fig. 3 shows the array patterns being normalized to the broadside gain when the scanning angles are $0°$, $+20°$, $+40°$, and $+60°$, respectively. As noted, the peak gain of one specifically beam-steered array pattern is proportional to the element gain at its main beam angle. As a consequence, the array gain will drop dramatically at large scanning angles if the element pattern has a narrow half-power beamwidth (HPBW).

In order to mitigate large gain drops at large scanning angles, the element pattern is expected to have a broad HPBW. This can be verified through a beam scanning array reported in [47]. Its element antenna has HPBWs of $93°$ and $113°$ in the E-plane and H-plane, respectively. The array configuration with this element exhibited a 4.7 dB gain decrease with respect to the broadside gain when scanning to $+45°$ in the E-plane. Whilst the gain decreases only 2.3 dB when the beam is scanned to $+45°$ in the H-plane.

The second issue is the mutual coupling among PAA elements. It is known that array elements are usually spaced at a relatively small distance (around 0.5λ) to avoid appearance of the grating lobes when the main beam is scanned. With a small element space, the radiation characteristics of one element in the array would be generally affected by the electromagnetic environment consisting of all the other elements. This phenomenon is called mutual coupling effect. The mutual coupling will not only affect the beam shape of the element pattern, but also cause its impedance matching to deteriorate. Moreover, the impedance characteristics would be varied with a dependence on the beam scanning angles. As a result, it would be a formidable task to match the impedance in a wide scanning angle range. Scan blindness is a common issue that occurs for WABS PAAs [48].

The third factor that should be carefully handled is grating lobes. Although the grating lobe can be avoided by setting a relatively small element spacing, a large element spacing is inevitable in some particular applications. These include the size of the element antenna being larger than half a wavelength, the mutual coupling effect being severe when the spacing is smaller than half a wavelength, etc. With a large spacing, the grating lobe may appear in the visible

region especially when the array beam is scanned to large angles. Thus, suppressing grating lobe is of great importance to increase array gain and efficiency [45]. Theoretically, to avoid grating lobes in a uniformly linear or rectangular-distributed planar array, the element spacing d should meet

$$d \leq \frac{\lambda}{1 + |\sin\theta_{max}|} \qquad (2)$$

where θ_{max} is the maximum scanning angle. If θ_{max} is anticipated to be $60°$, d should be maintained smaller than 0.53λ. Otherwise, grating lobes will appear in the visible region. Special techniques should thus be introduced to suppress grating lobes when a larger spacing is used.

The above challenging issues have attracted great research efforts along with significant advances for WABS PAAs. In the following sections, we will review and discuss the latest developments.

IV. WIDE-BEAMWIDTH ELEMENT ANTENNA

A number of innovative studies have been reported to maximize the beam scanning range of PAAs by developing and employing broad-beam antenna elements. There are two main antenna types being reported to facilitate the element pattern with wide beamwidth. The first type is passive single-port element antennas, and their beamwidths are intentionally broadened by sacrificing directivity and gain. This is comprehensible given the fact that the beamwidth is generally inversely proportional to the gain/directivity of the antenna. The other type is beam switchable element antennas. These include pattern reconfigurable element antennas and multi-port element antennas. Using this technique, the overall coverage of those available beams will become very large even though the beamwidth of each pattern is not wide. However, the switching will increase the cost and complexity, and there exists time delay for beam switching. In this section, we will review and discuss these two types of wide-beamwidth antenna elements.

A. WIDE-BEAMWIDTH PASSIVE SINGLE-PORT ELEMENT ANTENNA

We will mainly discuss two popular techniques to realize the wide-beamwidth passive single-port element. These include image theory-based element antenna and multimode element antenna. In addition, we will also briefly introduce some other methods for achieving passive wide beamwidth.

1) IMAGE THEORY BASED-ELEMENT ANTENNA

Generally speaking, an electromagnetic image antenna consists of an electric source positioned above a large perfect electric conducting (PEC) ground plane, or a magnetic source positioned above a large perfect magnetic conducting (PMC) ground plane. Owing to the inherent wide beamwidth nature of these electric/magnetic sources as well as the introduced proper imaging effect, the antenna beamwidth will be very broad. This technique is quite popular and has
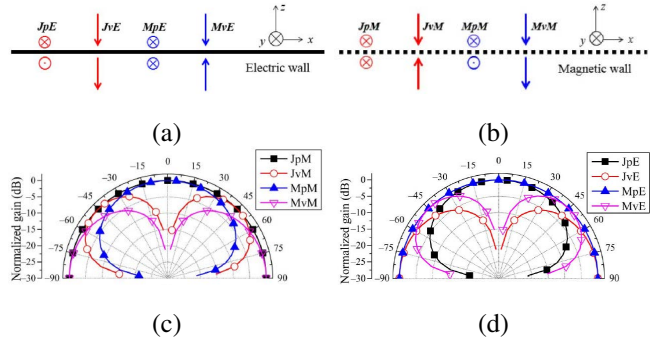
FIGURE 4. Eight basic types of image based antennas with (a) a PEC ground and (b) a PMC ground, and the corresponding theoretical radiation patterns (c) and (d) [49].
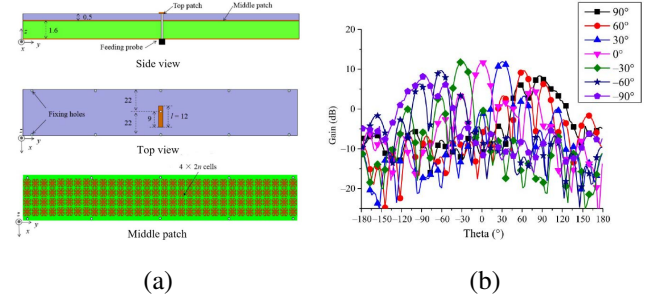

FIGURE 5. Geometry of the AMC-backed dipole antenna (a), and (b) the scanning patterns of the constructed 11-element linear array at 5.8 GHz in [49].
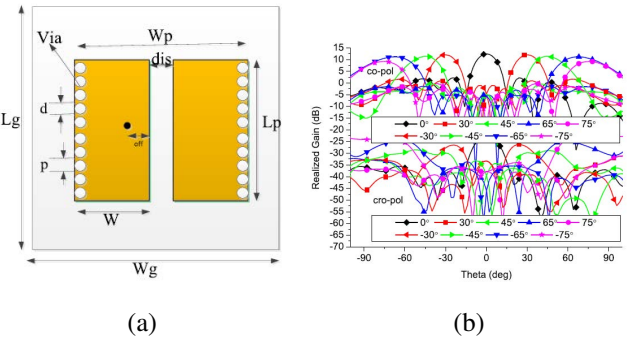

FIGURE 6. Structure of the developed magnetic dipole antenna (a), and (b) the measured WABS radiation patterns for the constructed 9-element E-plane array in [55].

been widely reported in [13], [49]–[56]. In the image-based antenna, the radiator can be equivalent to electric current J or magnetic current M; the ground plane has the PEC type and PMC type; the relative orientations of the radiator with reference to the ground plane can be parallel or perpendicular [49]. By using different combinations of the radiators and the ground planes, one can obtain eight basic antenna types. These eight types of antennas and their theoretical patterns are shown in Fig. 4. Take the MpE-antenna as an example, the "M" indicates the radiator is an equivalent magnetic current; "p" means the relative position is parallel; "E" indicates that the ground plane is PEC. Among the eight types of antennas, the radiation patterns $F(\theta)$ of the MpE- and JpM- antennas can be expressed as [49]:

$$F(\theta) = \cos(k_0 H \cos \theta) \qquad (3)$$

where H is the distance between the equivalent current source and the ground plane. As inferred from (3), the radiation patterns of MpE- and JpM- antennas are omnidirectional in the upper-half space as shown in Fig. 4(c) and (d). They are ideal candidates for serving as the element of WABS arrays.

An artificial magnetic conductor (AMC) backed antenna was designed as a JpM-type antenna in [49] to achieve WABS. As shown in Fig. 5(a), the antenna is equivalent to a dipole above an AMC ground. The HPBW of this antenna element in the H-plane is about $160°$, covering almost the whole upper half space. Subsequently, an 11-element array was constructed, and it achieved a wide angle beam scan from $-89°$ to $+90°$ in the H-plane, as shown in Fig. 5. In [50], besides WABS, the JpM AMC-backed dipole antenna was further improved to reduce the radar cross section (RCS) of the antenna array.

The MpE-type antenna can be constructed by simply placing a slot antenna on a large PEC ground plane (also known as magnetic dipole antenna) [13], [52]–[56]. For example, Liu *et al.* developed a microstrip magnetic dipole antenna with an omnidirectional radiation pattern in the upper half-space for WABS in [55]. The antenna configuration is shown in Fig. 6(a). An equivalent magnetic current source was created through the gap between the two pads, and an MpE-

type antenna was obtained. Then, an E-plane and an H-plane array were respectively constructed with this MpE-type element. For the E-plane array, the main beam was scanned from $-76°$ to $+76°$ as shown in Fig. 6(b). On the other hand, a beam scanning range from $-64°$ to $+64°$ was achieved for the H-plane array. As later reported by the same research group, the MpE-type element was miniaturized by developing an optimized wire antenna with a significantly reduced width [56]. The modified antenna achieved equivalent magnetic current performance. Subsequently, a 9-element linear array was constructed using the wire antenna, which enabled a beam scanning range from $-75°$ to $+75°$.

2) MULTIMODE ELEMENT ANTENNA
Rather than using a single mode for radiation, the multimode element antenna can excite and combine several resonant modes to realize a broadened beam [57]–[63]. A wide-beam microstrip antenna with metal walls that works at 3.2 to 3.8 GHz was reported in [57]. It consists of a U-slot patch antenna and vertical electric walls over the ground plane. A horizontal current is produced on the radiating patch, and a vertical current is induced on the electric walls driven by E-fields of the patch antenna, as can be seen in Fig. 7(a). A broadened beamwidth is achieved by combining the horizontal and vertical currents, as shown in Fig. 7(b). A 9-element H-plane scanning linear array and a 9-element E-plane scanning linear array were then constructed, which
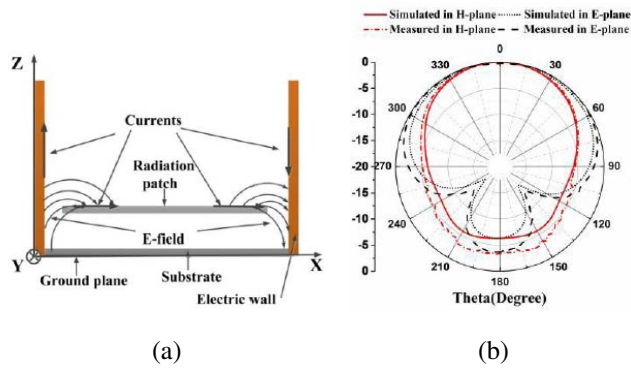
(a)   (b)

FIGURE 7. The antenna with vertical walls reported in [57] and its current distribution as well as radiation patterns. (a) shows side view of the antenna with the two types of currents. (b) shows the radiation patterns of this antenna.
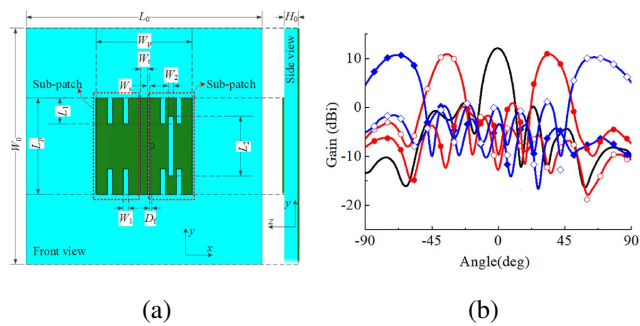

(a)   (b)

FIGURE 8. Geometry of the dual-mode antenna (a) reported in [61], and (b) the measured beam scanning patterns of the constructed 1×8-element linear array.

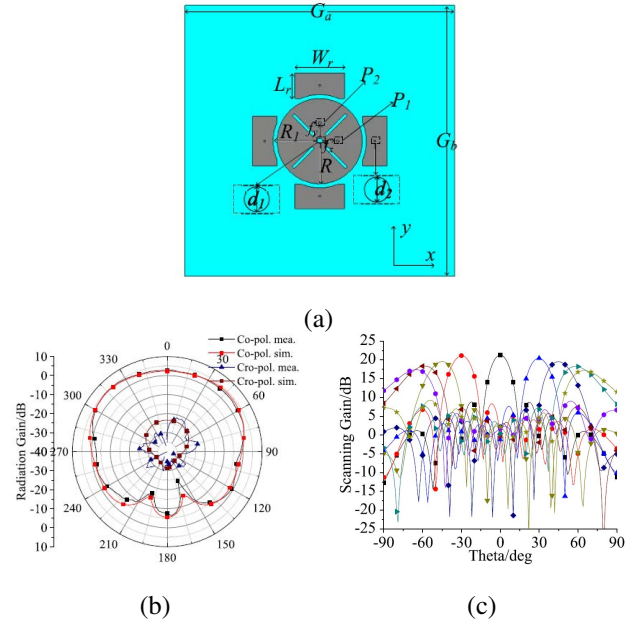(a)

(b)   (c)

FIGURE 9. Top view of the antenna (a) reported in [62], and (b) its radiation patterns as well as (c) the simulated beam scanning patterns of the constructed 8×8-element planar array at xoz-plane.

achieved a beam scanning range from $-90°$ to $+90°$ in the H-plane and from $-75°$ to $+75°$ in the E-plane. Other designs that achieve wide-beamwidth by inducing vertical currents using vertical electric walls or metallic strips were also reported in [58]–[60].

It is noticed that the method of introducing vertical currents will inevitably increase the profile of an antenna. To maintain a low profile, multimode patch antennas would be more preferred [61]–[63]. A single-fed hybrid-mode patch antenna was developed in [61] that achieved a wide beamwidth of $128°$. As shown in Fig. 8(a), a TM_{10} mode and TM_{20} mode can be excited at the left sub-patch and the whole patch simultaneously. When these two modes are combined, a wide-beam pattern is realized. An 8-element linear array was built with this antenna element, and a beam scanning range from $-68°$ to $+66°$ was achieved with gain fluctuation smaller than 1.5 dB, as shown in Fig. 8(b).

Besides the above developments, dual-polarization behavior that is necessary for some applications was incorporated into the wide-bandwidth antenna element in some reported works. A dual-polarized wide-beamwidth antenna element was reported in [62]. It consists of a circular patch and four rectangular parasitic patches distributed around the circular patch, as shown in Fig. 9(a). Dual polarization was realized by switching the feeding positions P_1 and P_2. A TM_{11} mode was excited in the circular patch, and a zero-order resonant

(ZOR) mode was excited in the parasitic mushroom-like rectangular patches. Ideally, an omnidirectional pattern will be obtained when these two modes are combined. This was validated by the simulated and measured patterns of this antenna as shown in Fig. 9(b). The developed wide-beam element was used to form an 8×8 planar PAA with 2-D WABS performance in [62], and a WABS range of about $\pm 65°$ in the two orthogonal planes with gain fluctuation less than ± 1.73 dB was achieved. The xoz-plane beam scanning patterns are shown in Fig. 9(c). Another dual-polarized antenna consisting of a mushroom-shaped patch and two circular patches employing the ZOR and TM_{010} modes was developed in [63]. The combination of the two modes achieved a radiation pattern with a wide coverage of up to $125°$. A 6×6-element planar PAA was designed using the developed antenna. Dual-polarized beam scanning was realized in a WABS range of $\pm 66°$ in both xoz and yoz planes with a scan loss of 3.5 dB.

3) OTHER METHODS

In addition to the aforementioned two popular methods, there are also some other techniques to accomplish wide-beamwidth passive antenna elements [64]–[72]. For example, a parasitic pixel layer-based antenna was reported in [65]. Fig. 10(a), (b), and (c) show the antenna configuration. It has two copper layers: a lower layer with an E-shaped patch and a ground plane; an upper layer with 4×4 small patches arranged periodically to pixelate the metal surface on the substrate. Strong coupling between the driven antenna and the parasitic surface induced large currents on the surface. In the parasitic surface, the connection between
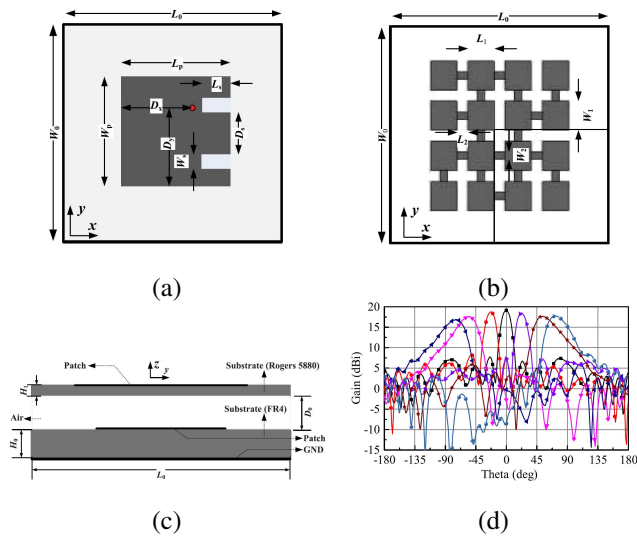
FIGURE 10. Structure of the reported antenna in [65] and the array beam scanning patterns. (a) Lower layer. (b) Upper layer. (c) Side view. (d) Beam scanning patterns of an 8×8-element array in xoz-plane.

FIGURE 11. The mode configurable antenna reported in [73] with PIN diodes to switch between TM_{01} and TM_{20} modes (a), element patterns for the two modes (b) and (c), and measured beam scanning array patterns using the two modes (d) and (e) for a 1×4-element array at 5.8 GHz.

these small patches was appropriately selected for wide-beam performance by using a co-simulation strategy with full-wave simulation and multi-objective optimization. It is shown that the HPBWs of the antenna are $188°$ and $156°$ in xoz- and yoz-planes. An 8×8-element planar array was then constructed, and it achieved a beam scanning range of $\pm75°$ in xoz-plane, as shown in Fig. 10(d).

Magnetic-electric dipole (ME-dipole) and Huygens sources are also effective in broadening the beamwidth of an antenna. For example, a circular polarized magnetic-electric dipole (ME-dipole) in [66] and a metamaterial-loaded DRA that integrates a pair of out-of-phase Huygens sources in [67] were presented for wide-angle beam scanning. Beam scanning ranges of $\pm66°$ and $\pm65°$ were achieved, respectively. A DRA with a saddle-shaped radiation pattern was developed in [68]. Its element pattern has a gain that is nearly inversely proportional to the peak gain of the array factor across a wide angular range and, consequently, the total array gain can stay almost identical in the whole scanning range. A 9-element linear array based on this DRA was designed, and a $\pm72°$ beam scanning was obtained. A hybrid topology optimization method was reported in [69] to optimize the shape of an patch antenna to achieve wide radiation beamwidth. For a 9-element linear array constructed with this element, a scanning range of $\pm80°$ was achieved.

Furthermore, high impedance surfaces (HISs) were deployed to realize the wide beamwidth in a low-profile fashion, as reported in [70]–[72]. A high-impedance periodic structure (HIPS) is proposed as a replacement for the traditional PEC ground of a U-slot loaded patch antenna in [71]. The HIPS results in an improvement in surface wave behavior, which in turn enhances the beamwidth of the antenna element pattern. The proposed antenna was used to form a 9-element linear array, which achieved a wide
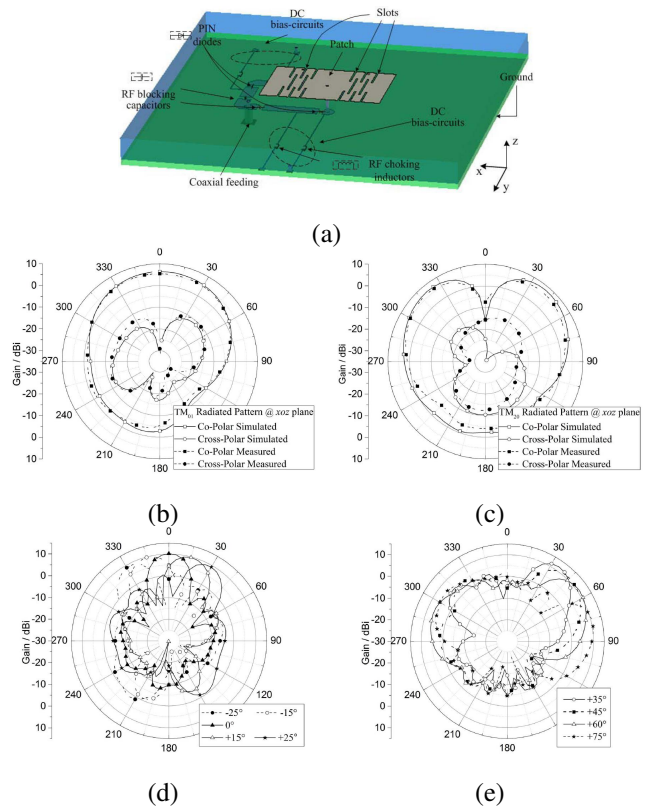
angle range of $\pm60°$ with only a 3.3 dB gain fluctuation. Mushroom-like HIS was used in [72] as the ground of a dipole antenna to broaden the element pattern beamwidth. The final array exhibits a wide scan angle up to $\pm85°$.

B. BEAM SWITCHABLE ELEMENT ANTENNA

Pattern reconfiguration is one commonly used method to actively achieve wide beamwidth for element antenna. A number of relevant works employing this technique have been reported [14], [73]–[85]. For example, a mode reconfigurable antenna employing PIN diodes working at 5.8 GHz was reported in [73]. It consists of a rectangular patch with 12 symmetrical slots for miniaturization and a reconfigurable feeding network, as shown in Fig. 11(a). By controlling the PIN diodes, the antenna can be switched between two different modes: TM_{01} mode with a broadside beam and TM_{20} mode with a conical beam, as respectively shown in Fig. 11(b) and (c). A 1×4 phased array was constructed with this element, and the array achieved a beam scan from $-75°$ to $+75°$ in the elevation plane with a gain fluctuation less than 3 dB, as shown in Fig. 11(c) and (d).

One can also use antennas with multiple individual feeding ports to excite different modes with complimentary patterns for wide beamwidth [14], [74], [75]. An overall broad-beam pattern with dual orthogonal polarizations was achieved in
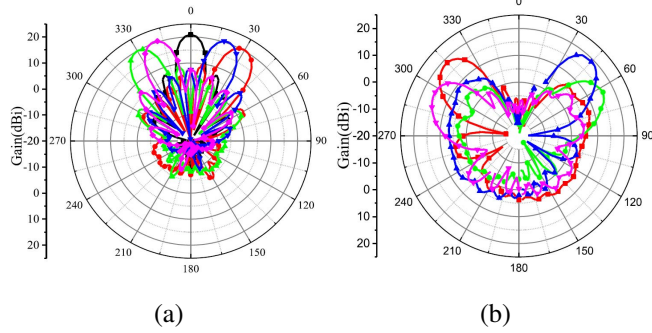
(a)   (b)

FIGURE 12. The measured beam scanning patterns in xoz-plane for a 8×8-element array reported in [74]. (a) Scanning performance using TM_{10} mode. (b) Scanning performance using TM_{21} mode.

(a)   (b)

FIGURE 13. Configuration of the pattern reconfigurable DRA (a), and (b) the beam scanning radiation patterns of the 1×4 linear array reported in [76].

[74] by combining three working modes: TM_{10} and TM_{01} modes by exciting a square patch and a TM_{21} mode by exciting the circular ring patch. An 8×8 planar array comprising of this element achieved a wide beam scanning range of $\pm 64°$ in two orthogonal planes, and the beam scanning patterns in xoz-plane are shown in Fig. 12. In [75], a windmill-shaped loop antenna backed with an HIS was developed. The antenna employed an upper and a lower substrate, and a mushroom-like HIS comprised of rectangular patches and shorted vias was placed at the back of the lower substrate to eliminate the back radiation with reduced aperture. The antenna realized independently directed tilted beams by using four different excitation ports. A 4×4-element array was constructed with this antenna, and it was capable of scanning its main beam up to $+72°$ in elevation in each of the four spatial quadrants.

Note that the above multi-port antennas individually excite each port for a special beam pattern. By switching the excitation port, different beam patterns can be chosen and, hence, an overall wide beamwidth is obtained by combining all these operating states. An alternative method that manipulates the phases for multiple excitation ports can also achieve wide beamwidth [76], [77]. A dual-port pattern-reconfigurable antenna was reported in [76], as shown in Fig. 13(a), that uses reconfigurable phase shifters for beam reconfiguration. The pattern reconfiguration was achieved by exciting the two ports with phase differences of $-90°$ and $90°$, respectively. The final four-element PAA achieved a scanning range of $\pm 162°$ with a gain fluctuation of 1.25 dB, as shown in Fig. 13(b). In addition, other investigations reveal that wide-angle beam scanning can be realized in several cutting planes [78], [80], [81]. A dielectric resonator antenna with eight reconfigurable horizontally tilted beams was developed in [78]. A $\pm 60°$ beam scanning in multiple planes of $\phi = 0°$, $45°$, $90°$, and $135°$ was achieved by a 4×4-element array of the designed antenna.

C. BRIEF SUMMARY
Based on the above discussions on the wide beamwidth element antenna technologies, the following findings can be summarized when comparing beam switchable antenna
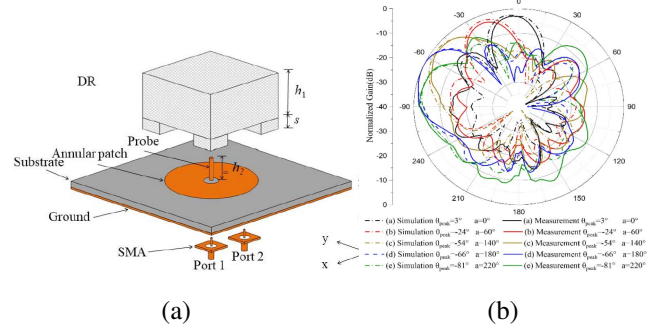
elements and passive broad-beam single-port ones in the context of WABS. Passive broad-beam elements exhibit the benefits of a simple feeding network and easy implementation. However, they generally have lower gains due to the trade-off made to achieve wider beamwidth. In contrast, beam switchable elements can provide higher gains but require additional control components or techniques for beam switching, such as PIN diodes. Therefore, the selection of antenna element can be determined based on custom-designed requirements for achieving WABS PAAs.

V. MUTUAL COUPLING IN WIDE ANGLE PAA
Mutual coupling has a large effect for array beam scanning performance, especially at large angles. It is a crucial issue that should be carefully handled for WABS PAA [86]. Generally, there are two main methods to deal with mutual coupling issues: The first is considering, optimizing, and utilizing mutual coupling in the element design and the resultant PAA with this element can be naturally suitable for WABS. The second is to mitigate the mutual coupling among antenna elements and, hence, the mutual coupling effect can be negligible during WABS. In the following, we will discuss these methods and the associated antennas reported in the literature in detail.

A. MUTUAL COUPLING BASED OPTIMIZATION
When mutual coupling exists in the PAA, the coupling coefficients generally vary when the array main beam scans to different angles. This is because the changing rate of active input susceptance at a high beam-steering angle is generally faster than that of the admittance during the beam scanning [87]. Therefore, implementing a wide-angle impedance matching (WAIM) layer to compensate for this difference is an effective method that can optimize the impedance matching in a very large angular range.

Many designs using pure dielectric or metasurface super-strates have been developed, such as those in [87]–[89], to realize WAIM. For example, a unit cell with a perforated dielectric sheet working as a WAIM layer was reported in [87]. The unit cell consists of a Vivldi-like antenna and a perforated WAIM, as shown in Fig. 14(a). A 16×16-element
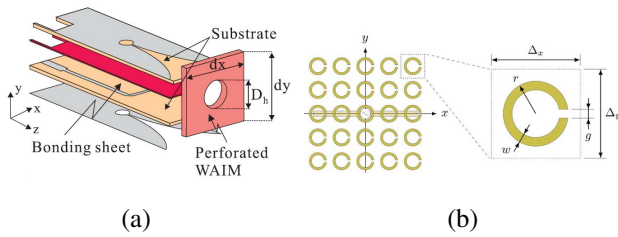
(a)   (b)

FIGURE 14. Structures of the unit cells with dielectric WAIM layer reported in [87] (a), and (b) the metasurface WAIM layer with split rings reported in [88].

(a)   (b)

FIGURE 15. Structure of the tightly coupled dipole array (TCDA) unit cell with a metasurface WAIM layer reported in [96] (a), and (b) the VSWRs of an center element in a 16×16-element planar array for different scanning angles.

array was formed with this unit cell. When the beam was scanned to $70°$ in the E-plane and H-plane, the array showed an active S-parameter characteristic of less than -9.13 dB. The gain decreased by 3.83 and 2.87 dB for the E-plane and H-plane scanning, respectively. Fig. 14(b) shows the unit cell employing a metasurface WAIM layer with split rings reported in [88]. It has been demonstrated that, comparing to dielectric WAIM or the case without WAIM layer, this metasurface WAIM can increase the scan range in the D- and H-planes by $16°$ and $10°$, respectively, while having a negligible impact in the E-plane.

Despite their outstanding performance in WABS, the above antenna arrays cannot achieve a very wide operating bandwidth. Further investigations were carried out to improve the bandwidth of WABS PAA. Tightly coupled antenna arrays (TCAAs) technology exploits the strong coupling capacitance between the array elements to counteract the inductive effect of the ground on the antenna. This way a wide bandwidth even ultra-wideband (UWB) operation can be obtained.

Electrical dipole is a popular unit structure being employed in TCAAs [90]–[107]. For example, in [96], a balanced antipodal dipole was designed for UWB and WABS tightly coupled dipole array (TCDA). The unit configuration is shown in Fig. 15(a). As noted, a metasurface WAIM is placed above the dipole to achieve a wider angle scanning characteristic while maintaining a low profile. A 16×16-element planar array was formed with this unit. Fig. 15(b) shows the attained VSWRs of the center element when the array has its beam scanned to different angles. Simulated and measured results verified that the developed TCDA was able to operate over a 5:1 bandwidth with active VSWR < {2, 2.8, 3.2} for scanning to {broadside, $45°$, $60°$}, respectively. In [97], a millimeter-wave (mmWave) TCDA operating in a wide bandwidth from 23.5 to 29.5 GHz was realized. It achieved a beam scanning up to $\pm 60°$ in E-, H-, and D-plane within the whole operating band.

B. MUTUAL COUPLING MITIGATION

Rather than optimizing the mutual coupling between array elements, one can mitigate the mutual coupling and, hence, alleviate the mutual coupling effect for WABS PAAs. Several interesting methods have been reported to achieve this objective.
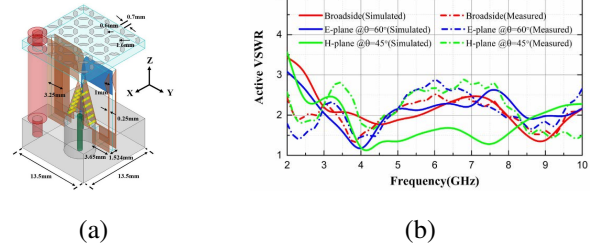
Electromagnetic bandgap (EBG) structures are generally 3-D periodic objects that prevent the propagation of electromagnetic waves in a specified band of frequency for all angles and for all polarizations [108]. Thus, electromagnetic bandgap (EBG) structures are effective in reducing mutual coupling and improving the WAIM since propagation of the surface waves in the bandgap of EBG can be suppressed due to high surface impedance [109]. A wideband wide-beam scanning PAA with cavity-backed antennas was developed in [110]. The detailed antenna structure with the EBG is shown in Fig. 16(a) and (b). The element was fed by a microstrip line through a feed patch with a backed cavity. Four narrow strips on a suspended thin substrate were placed at the top surface to obtain the best impedance matching over the entire frequency band. Mushroom-like EBG structures were utilized to suppress the E-plane scan blindness caused by the surface waves. A 13×5 triangular distributed planar array was exampled. Good impedance matching was achieved at different scanning angles within the operating band of $7 - 13$ GHz. The active VSWRs of a center element for different scanning angles are shown in Fig. 16(c), and the beam scanning patterns in E-plane at 10 GHz is provided in Fig. 16(d).

Defected ground structure (DGS) is another commonly used strategy for achieving WAIM by reducing the mutual coupling [111]. By employing the DGSs, a metasurface-based antenna was reported in [112] to achieve WABS. Fig. 17(a) shows the slot-fed grid square patch metasurface antenna array. The DGS was realized by the meander-line slots etched on the ground plane. Benefiting from the DGS, the scanning range was much improved without increasing any dimension. The array can scan its main beam to a maximum angle of $50°$ at the 5.2 GHz, as shown in Fig. 17(b). Moreover, enhanced scanning capabilities can be obtained over the wide frequency band from 4.6 GHz to 5.8 GHz. Besides, in [113], a metasurface antenna with DGSs for scanning blindness suppression and impedance matching improvement was reported. It realized an 8×8 metasurface PAA with $\pm 60°$ beam scanning range and impedance bandwidth of 22.2%.

Apart from the above effective methods for mutual coupling mitigation, a concept of array-antenna decoupling
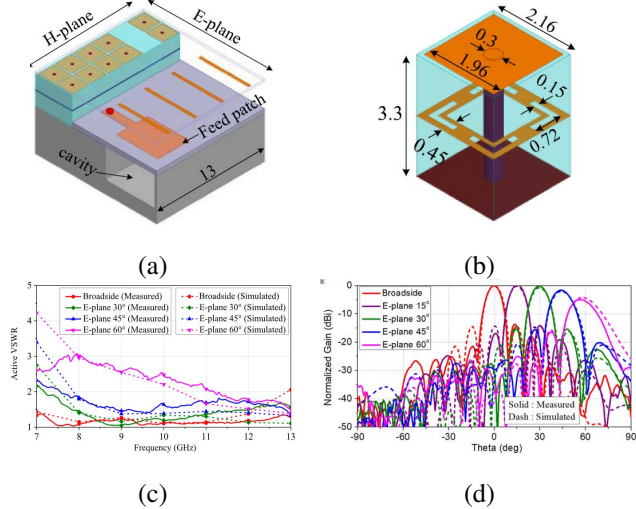
(a)

(b)

(c)

(d)

FIGURE 16. Geometries of the reported unit with EBGs and the corresponding element and array performances [110]. (a) 3-D view of the unit, (b) 3-D view of the EBG unit, (c) measured and simulated active VSWRs of a central element, and (d) the E-plane scanning patterns of a 13×5-element triangular-distributed array at 10 GHZ.
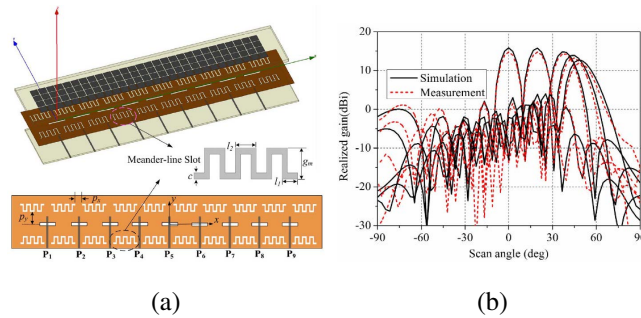

(a)

(b)

FIGURE 17. Configuration of the developed 1×9-element metasurface antenna array with DGSs (a), and (b) the corresponding scanning patterns in [112].
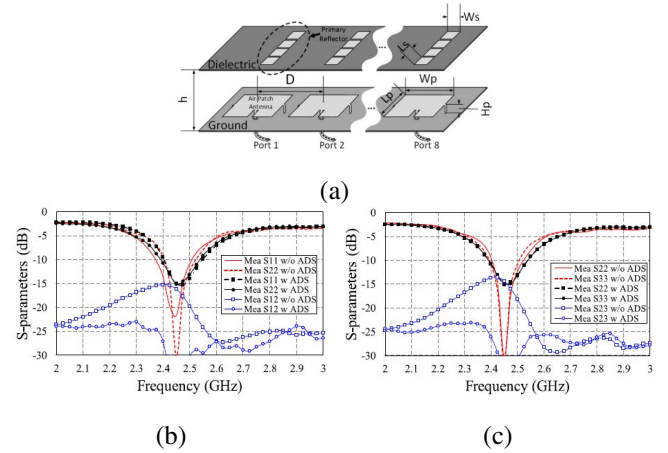

(a)

(b)

(c)

FIGURE 18. Eight-element patch antenna array with a designed ADS for mutual coupling reduction (a) and the representative measured S-parameters of the array with and without the ADS of (b) antennas 1 and 2 and (c) antennas 2 and 3 [114].

In addition, some other technologies such as the metasurface slabs [115], reactive impedance surfaces [116], and frequency selective surfaces (FSSs) [117] have been reported to suppress the mutual coupling for WABS.

C. BRIEF SUMMARY

In relation to the above review, it is noted that the mutual coupling based optimization method is widely employed to facilitate WABS PAAs. This method can effectively incorporate and leverage mutual coupling for achieving WABS PAA. Furthermore, additional performance features such as wide operating bandwidth can be generated by optimizing the mutual coupling, as demonstrated by TCAAs. However, this optimization may result in a higher profile due to the introduction of WAIM layers. Regarding the mutual coupling mitigation method, employing an EBG or a DGS structure can maintain a lower profile for the PAA. However, when employing other mutual coupling mitigation techniques involving ADS, metasurface slab, reactive impedance surface, and FSS, the profile still remains an issue. It is clear that the method chosen for the WABS PAA would differ depending on whether the objective is to obtain a wide bandwidth or maintain a low profile.

VI. GRATING LOBE CANCELLATION

In most practical applications, grating lobes should be avoided since they generally cause unwanted radiations, thereby degrading the gain and efficiency of the PAA [118]. As previously analyzed, grating lobes would appear especially when the beam is scanned to large angles. It is common knowledge that an array pattern is the product of the element pattern and array factor. Therefore, to eliminate the grating lobes of WABS PAA, two main methods have been widely implemented: one is employing nonuniform or triangular-latticed element distributions in the aspect of the array factor; the other revolves around the element pattern

surface (ADS) was developed in [114]. The ADS is a thin layer of low-loss and low dielectric constant substrate printed with a plurality of electrical small metal reflection patches. These reflection patches are carefully designed to create diffracted waves at the coupled antenna port to cancel the coupled waves meanwhile minimizing the perturbation to the original array antenna. The distance between the ADS and the ground plane of the array antenna is determined to make sure the diffracted wave is out of phase with respect to the coupled waves from the coupled antenna element port. Design guidelines and considerations of the ADS were discussed in [114], and two practical design examples were provided to evaluate the ADS. Fig. 18(a) shows the configuration of one exampled PAA. The representative S-parameters of antenna elements in the array with and without the ADS are given in Fig. 18(b) and (c), respectively. It is seen that the mutual coupling between any two adjacent elements, i.e., S_{12} or S_{23}, is significantly reduced from about -15 dB to below -30 dB, which has demonstrated the good performance of the ADS in reducing the mutual coupling.
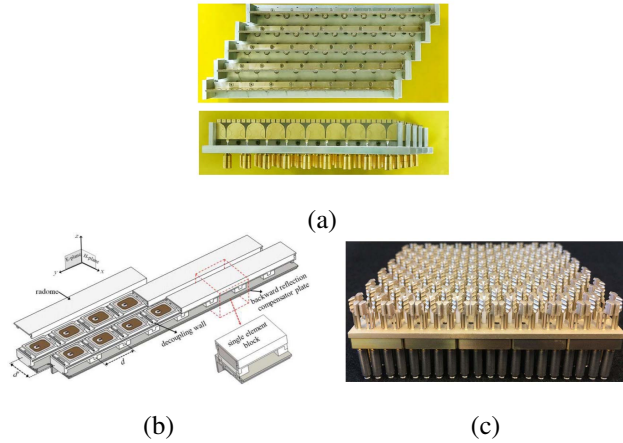
FIGURE 19. WABS Arrays with triangular latticed elements for avoiding the grating lobes. (a) a 5×9-element array presented in [116], (b) a 2×8-element array-element array presented in [119], and (c) a 12×20-element array presented in [121].

aspect and entails the use of antenna elements with pattern nulls precisely positioned at the grating lobe directions.

A. GRATING LOBE CANCELLATION METHODS

Using triangular-latticed array layout is a simple but effective way to avoid grating lobes. Compared to rectangular-latticed array, the triangular-latticed one has a enhanced spacing range that is free from the grating lobes apart from the advantage of element number reduction. To avoid grating lobes, the element spacing in an triangular-latticed array should meet [45]

$$d_x \leq \frac{1}{\sin \alpha} \cdot \frac{\lambda}{1 + |\sin \theta_{max}|} \quad (4)$$

$$d_y \leq \frac{1}{\cos \alpha} \cdot \frac{\lambda}{1 + |\sin \theta_{max}|} \quad (5)$$

where

$$\pi/6 \leq \alpha \leq \pi/3 \quad (6)$$

is the basic angle of the isosceles triangle in the triangular grid, d_x and d_y are element spacing in two dimensions, and θ_{max} is the maximum scanning angle. As indicated from (4) and (5), assuming $\theta_{max} = 60°$ is anticipated, the element spacing d_x and d_y should be maintained smaller than 0.76λ when $\alpha = 45°$. The value of 0.76λ is 0.23λ larger than that for the rectangular layout. Many interesting PAAs have been presented to achieve WABS by employing triangular-latticed layouts [87], [110], [116], [119]–[121]. Some examples of them are shown in Fig. 19. They can generally achieve beam scanning ranges no less than $60°$ with gain degradation smaller than 3 dB.

Employing a nonuniform element distribution is also effective method to alleviate the grating lobes. Such method can break the periodicity and redistribute the energy in the grating lobes throughout the far field pattern [122]. Many effective methods have been proposed to mitigate the grating lobes by employing nonuniform or sparse element spacing

[123]–[126]. For example, in [123], the genetic algorithm is employed to achieve thinned aperiodic linear PAAs to suppress the grating lobes with increased steering angles. The optimized array can achieve a beam scanning angle of $60°$ with constrained SLLs.

Another popular method for grating lobe cancellation is employing antenna elements with nulls or low power at the grating lobe directions [127]–[130]. In [127]–[129], dual-mode antenna elements were designed to achieve element patterns with main beams at the anticipated scanning region and low power at the grating lobe directions. For example, in [129], a dual-mode antenna consisting of a square DRA with $TE_{1\delta1}$ mode and a monopole with TM_{101} mode was designed. These dual modes were excited with two individual ports. The radiation patterns of the dual modes are shown in Fig. 20(a). By exciting the dual modes simultaneously with identical amplitudes but a phase difference of $\delta_{01} = 180°$, as shown in Fig. 20(b), the overall element pattern with a peak in the scanning angle meanwhile a low power in the grating lobe direction was achieved. With this dual-mode antenna, a 1×4-element linear array with an inter-element spacing of 0.95λ was constructed. Fig. 20(c) and (d) show the beam scanning patterns. As is seen, grating lobe is well canceled by adopting the antenna element.

In addition, a null scanning antenna with varactor loaded impedance reconfigurable circuits was developed in [130]. The exploded view of the designed antenna is shown in Fig. 21(a). The antenna can provide continuous null scanning for grating lobe cancellation as well as desired main beam steering in two orthogonal planes. The beam scanning of the antenna element pattern along with the array pattern for a 4×4-element 0.8λ-spaced planar array are shown in Fig. 21(b). Array factor without element pattern is also provided for comparison. It is shown that, by adopting this antenna element, the grating lobe can be effectively suppressed during the scanning by keeping the null always at the grating lobe direction.

B. BRIEF SUMMARY

In summary, achieving grating lobe cancellation can be approached from the perspective of either the element pattern or the array factor. From the array factor perspective, both nonuniformly-spaced and triangular-latticed layouts are effective methods. The former method may require a more complicated feeding network while the latter one can simplify the feeding network. However, the grating lobe cancellation effect is comparatively limited with the triangular-latticed layout. Regarding the element pattern perspective, using beam switching antenna elements with null patterns can effectively suppress the grating lobe. However, the introduction of PIN diodes or varactors can lead to additional losses and reduced efficiency. The associated biasing network will also be complex. Interested readers should carefully evaluate these factors and select appropriate techniques for grating lobe cancellation in WABS PAAs.
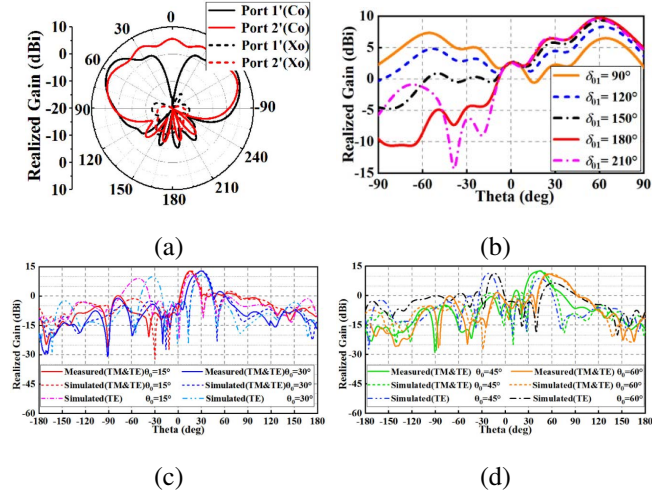
FIGURE 20. Radiation patterns of a dual-mode element and the beam scanning patterns of a 1×4-element 0.95λ-spaced linear array in [129]. (a) radiation pattern of the dual mode (TE and TM modes) antenna. (b) the element patterns when its two modes are fed with equal amplitudes but different phase differences. (c) and (d) show the array pattern with scanning angles of $15°$, $30°$, $45°$, and $60°$ with grating lobe cancellation. Patterns with the elements all working at TE mode are also shown for comparison.
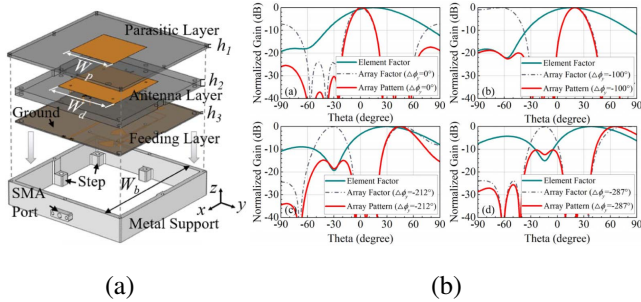

FIGURE 21. The null scanning antenna as well as the element and array patterns presented in [130]. (a) exploded view of the null scanning antenna, and (b) the element pattern and array patterns of a 4×4-element 0.8λ-spaced planar array with different scanning angles. (b) also shows the array factor with isotropic element pattern as a comparison.

VII. FREQUENCY SCANNING PAA FOR WIDE-ANGLE BEAM SCANNING (WABS)

We have thoroughly discussed the electronically controlled PAAs for WABS in the previous sections. As reported, the electronically scanned PAAs showed attractive radiation and impedance performance with great flexibility. However, those performance generally need to use many phase shifters to controlling the excitation phases of all the elements. As a consequence, the complexity as well as the system cost is greatly increased. To this end, frequency-based beam scanning is a promising choice for low-cost beam scanning systems. They do not rely on any phase shifters for beam scanning. In contrast, they achieve beam scanning by changing the source frequency of the PAA. It is evident that the frequency scanning PAA has many significant advantages such as being simple, easy for fabrication, and low-cost. This makes the frequency scanning PAA being attractive for many modern applications including imaging systems and direction
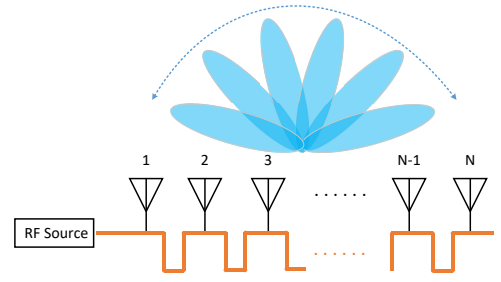

FIGURE 22. A schematic view of the leaky-wave antenna for WABS.

finding networks [131], [132]. It is also acknowledged that owing to the dependence on the operating frequency, the freedom for beam scanning is much reduced in comparison to that with phase shifters. This may lead to performance degradation for frequency scanning PAAs compared to the electronically controlled PAAs. Moreover, the variation of frequency at different beam angles prohibits the PAA application in many systems such as most communications systems. Therefore, there is a trade-off between the system cost and the performance characteristics.

Fig. 22 shows a systematic view of the leaky-wave antenna (LWA), one typical type of the frequency scanning PAA, for WABS. The LWA employs guiding structures to support wave propagation, and the electromagnetic energy is gradually radiated or leaked with the wave traveling along the waveguiding structures [133]. The guiding wave is represented by the long connected line and the radiators can be treated as an array of individual antenna elements, as seen in Fig. 22. Thus, the LWA is equivalent to a series feed antenna array. For one-dimensional (1-D) LWA, the main beam angle θ can be obtained through the following relation [134], [135]:

$$\theta(f) = \sin^{-1} \frac{\beta(f)}{k_0(f)} \quad (7)$$

where β is phase constant in the waveguiding structure. Generally, the traveling wave has an inherent dispersion, which contributes to a frequency-based beam scanning for 1-D LWA. For example, an 1-D slot array LWA was reported in [136] as shown in Fig. 23(a). It has both longitudinal and transverse slots and is loaded with an array of shorting vias in each unit cell. By sweeping the operating frequency band ($|S_{11}| \leq -10$ dB) from 8.5 to 14.4 GHz, the antenna achieved a measured beam scanning range from $-53°$ to $+37°$, as observed in Fig. 23(b) and (c).

To facilitate WABS with LWAs, there are several critical challenges. The first is an open-stop band (OSB) issue. The OSB is caused by the reflection from each unit cell adding up in-phase at the input port when the beam points towards the broadside direction [137]. It leads to deteriorated impedance matching and degraded gain. Therefore, the OSB effect prevents a continuous beam scanning through broadside for LWAs. To suppress the OSB, researchers have developed numerous techniques, including utilizing composite right/left
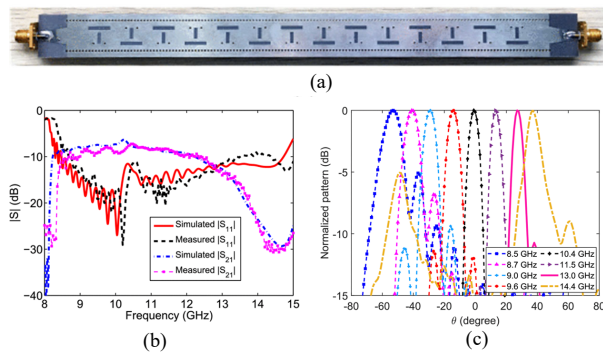
FIGURE 23. 1-D slot array leaky-wave antenna reported in [136]. (a) The fabricated antenna prototype. (b) Simulated and measured S-parameters. (c) Measured beam scanning radiation patterns.
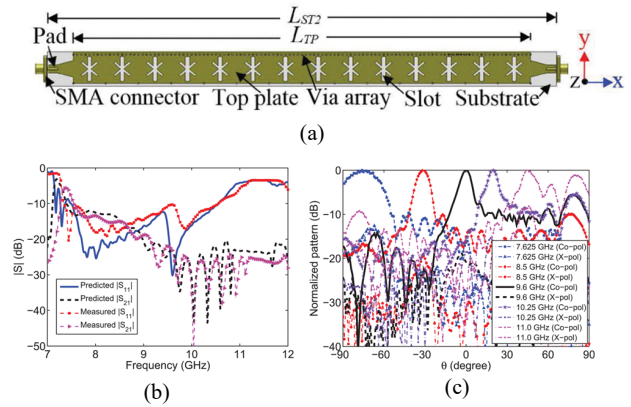

FIGURE 24. Slotted SIW LWA with partially reflecting vias and its performances reported in [131]. (a) The fabricated antenna prototype. (b) Simulated and measured S-parameters. (c) Measured beam scanning radiation patterns.

handed (CRLH) structures [136], [138]–[141] and employing impedance matching methods [142]–[144]. The second are those difficulties we have introduced and discussed for the electronically scanned PAA in the previous sections. For example, one needs to realize wide element pattern beamwidth to compensate for gain losses at large angles and maintain wide-angle impedance matching to avoid large gain variations.

To date, a variety of techniques have been reported to overcome the above challenges and, hence, to facilitate LWAs with frequency-based WABS. A slotted SIW LWA with partially reflecting vias was reported in [131], and its configuration is shown in Fig. 24. Unlike the conventional SIW with two closely-spaced via walls (acting as PEC walls), the developed antenna has one via wall sparsely distributed for OSB suppression. The specified-shaped slot was used and optimized to improve the linear polarization purity. Fig. 24 shows the simulated and measured S-parameters. It is seen that the OSB was mitigated and a wide operating wide was obtained. By sweeping the frequency from 7.625 to 11 GHz, the main beam was scanned from $-74°$ to $+45°$, a total range of $119°$. As revealed in [132], the beam scanning range can be further increased, being from $-76°$ to $+67°$. This was accomplished by employing a combination structure of composite right/left-handed (CRLH) lines, magnetic dipole, and alumina ceramic block. Note that these WABS LWAs can't point towards endfire directions. One main reason is the effect caused by the ground plane. In this regard, those ground-free structures are promising to further enhance the beam scanning range from backward to forward and further to endfire directions. Various techniques including the Goubau line [145], [146] and spoof surface plasmon polariton (SSPP) [147]–[149] were reported to achieve that goal. In [148], double-layer glide-symmetric spoof surface plasmon polaritons (SSPPs) structures were developed that scans the beam from $-90°$ to $+44.3°$. The attained realized gain ranges from 8.03 to 12.17 dBi. Besides the elevational beam scanning as reported by the above WABS LWAs, the periodic co-planar-strip LWA reported in [150] realized an

azimuthal beam scanning range from $-75°$ to $+84°$. The azimuthal directed beam was obtained by using open-ended slots.

VIII. DISCUSSION AND FUTURE SCOPE

In Section III, we discussed the main challenges in facilitating WABS. In Sections IV, V, and VI, we conducted a comprehensive review of the existing literature, presenting various techniques to address these challenges. Notably, we did not distinguish between linear and planar arrays in those discussions. This is because both types of arrays face similar challenges, and the techniques employed to tackle these challenges are also comparable. For example, both linear and planar arrays need to be cautious of the appearance of grating lobes as the element spacing increases. They also need to address mutual coupling issues, particularly at large scanning angles, and require antenna elements with relatively wide beamwidths for WABS. A slight difference is that mutual coupling in planar arrays is more severe than that in linear arrays. Furthermore, it is clear that planar arrays require the elements with wide beamwidths in dual or multiple cuts to achieve WABS in corresponding planes [65], whereas linear arrays only require wide beamwidths in one cut within the scanning plane.

Although WABS PAAs have achieved significant developments, there are several potential research challenges for future emerging systems with the evolution of wireless technologies. As discussed in Section IV, wide-beamwidth antenna elements are commonly utilized for WABS with small gain decrease at large angles. However, this wide-beamwidth element generally has a narrow bandwidth and, hence, the associated PAAs are also narrow-band [151]. Further efforts are needed to increase their bandwidths to broaden their areas of application. In addition, regarding the method of using beam switchable element, complex control and additional losses are unavoidable due to the involvement of switching devices/ports, as previously mentioned.

Therefore, future research should aim to minimize the losses and complexities. Potentially, the element can be optimized to locate the switching devices in small-current areas while maintaining beam switching performance.

Tightly coupled arrays are generally used to achieve wideband or ultra-wideband WABS. These arrays typically require wideband feeding structures, like baluns, and impedance matching layers. This may lead to bulky configurations and high profiles. Further work is expected to optimize the configuration into an integrated and compact structure.

The future B5G and 6G communications demands antenna arrays that operate at mmWave and even higher frequencies to support high data rates and to achieve low latency. However, compared to their lower frequency counterparts, there has been limited research on mmWave and even higher-band WABS PAAs. Higher frequencies pose new challenges due to the small physical sizes of antenna elements, which result in difficulties with manufacturing feasibility, assembly complexity, and beamforming network complexity [152]. Additionally, losses can be very high at mmWave frequencies. Therefore, future research on mmWave WABS PAAs should prioritize improving the efficiency, reducing costs, and addressing fabrication feasibility.

Multibeam antennas are regarded as a critical technology for B5G and 6G wireless communications networks. Achieving wide-angle scanning multibeams is an important research focus for the future. Analog beamforming networks, which offer advantages such as low cost and low energy consumption, have gained significant interest in recent years. A recently proposed solution, the generalized joined coupler (GJC) matrix, allows for independent scanning of multibeams [153], [154]. As such, GJC matrices hold great promise for achieving wide-angle scanning multibeams. However, research on GJC matrices is still in its early stage, and further research is necessary to enable continuous wide-angle scanning multibeams.

IX. CONCLUSION

This paper presented a thorough review of wide-angle beam scanning (WABS) phased array antennas (PAAs) in the literature. It is shown that there are three crucial factors that should be considered for a WABS PAA: the beamwidth of element pattern, mutual coupling among elements, and grating lobes. To tackle these challenges, a number of developed technologies with electronically scanned PAAs have been discussed in this review, including implementing a wide beamwidth element antenna with passive or active methods, optimizing the mutual coupling with wide-angle impedance matching (WAIM) or mitigating the mutual coupling, and suppressing grating lobes. Finally, WABS frequency scanned PAAs featuring easy for fabrication and low cost were also investigated. This timely review fulfills the need for a comprehensive investigation of WABS technologies for PAAs, providing a thorough and detailed introduction and guidance

for interested researchers and engineers. It is expected that the paper will stimulate further research and development on this important technology.

REFERENCES

[1] Y. J. Guo, M. Ansari, R. W. Ziolkowski, and N. J. G. Fonseca, "Quasi-optical multi-beam antenna technologies for B5G and 6G mmwave and THz networks: A review," *IEEE Open J. Antennas Propag.*, vol. 2, pp. 807–830, 2021.

[2] P. Castillo-Tapia, O. Zetterstrom, A. Algaba-Brázález, L. Manholm, M. Johansson, N. J. G. Fonseca, and O. Quevedo-Teruel, "Two-dimensional beam steering using a stacked modulated geodesic Luneburg lens array antenna for 5G and beyond," *IEEE Trans. Antennas Propag.*, vol. 71, no. 1, pp. 487–496, 2023.

[3] W. Hong, Z. H. Jiang, C. Yu, J. Zhou, P. Chen, Z. Yu, H. Zhang, B. Yang, X. Pang, and M. Jiang, "Multibeam antenna technologies for 5G wireless communications," *IEEE Trans. Antennas Propag.*, vol. 65, no. 12, pp. 6231–6249, Dec. 2017.

[4] S. Chen and J. Zhao, "The requirements, challenges, and technologies for 5G of terrestrial mobile telecommunication," *IEEE commun. mag.*, vol. 52, no. 5, pp. 36–43, 2014.

[5] Y. Feng, J. Y. Li, L. K. Zhang, X. J. Yu, Y. X. Qi, D. Li, and S. G. Zhou, "A broadband wide-angle scanning linear array antenna with suppressed mutual coupling for 5G sub-6G applications," *IEEE Antennas Wirel. Propag. Lett.*, vol. 21, no. 2, pp. 366–370, Feb. 2022.

[6] Y. Luo, J. Xu, Y. Chen, Y. Sun, B. Xu, S. Xu, and G. Yang, "A zero-mode induced mmwave patch antenna with low-profile, wide-bandwidth and large-angle scanning for 5G mobile terminals," *IEEE Access*, vol. 7, pp. 177 607–177 615, 2019.

[7] G. Yang and S. Zhang, "Dual-polarized wide-angle scanning phased array antenna for 5G communication systems," *IEEE Trans. Antennas Propag.*, vol. 70, no. 9, pp. 7427–7438, Sep. 2022.

[8] Z. Wang, Y. Dong, Z. Peng, and W. Hong, "Hybrid metasurface, dielectric resonator, low-cost, wide-angle beam-scanning antenna for 5G base station application," *IEEE Trans. Antennas Propag.*, vol. 70, no. 9, pp. 7646–7658, Sep. 2022.

[9] K. K. W. Low, T. Kanar, S. Zihir, and G. M. Rebeiz, "A 17.7–20.2-GHz 1024-element K-band SATCOM phased-array receiver with 8.1-dB/K G/T, ±70° beam scanning, and high transmit isolation," *IEEE Trans. Microw. Theory Tech.*, vol. 70, no. 3, pp. 1769–1778, 2022.

[10] A. H. Aljuhani, T. Kanar, S. Zihir, and G. M. Rebeiz, "A 256-element Ku-band polarization agile SATCOM receive phased array with wide-angle scanning and high polarization purity," *IEEE Trans. Microw. Theory Tech.*, vol. 69, no. 5, pp. 2609–2628, May 2021.

[11] X. Chang, H. B. Wang, T. J. Li, S. C. Jin, D. G. Liu, and Y. J. Cheng, "Shared-aperture phased array antenna with codesigned near-field coupled circular polarizer loaded for K/Ka-band wide-angle satellite communication," *IEEE Trans. Antennas Propag.*, vol. 70, no. 9, pp. 7478–7490, Sep. 2022.

[12] P. Schmalenberg, E. M. Dede, T. Nomura, and S. Nishiwaki, "Optimization of planar phased arrays for vehicles," *IEEE Antennas Wirel. Propag. Lett.*, vol. 21, no. 10, pp. 2140–2144, 2022.

[13] Z. Yi, R. Zhange, B. Xu, Y. Chen, L. Zhu, F. Li, G. Yang, and Y. Luo, "A wide-angle beam scanning antenna in E-plane for K-band radar sensor," *IEEE Access*, vol. 7, pp. 171 684–171 690, 2019.

[14] F. Peng, C. Liao, Y. F. Cheng, and L. X. Guan, "A multi-mode pattern reconfigurable antenna with wide beam coverage and its application to dual-polarized wide-angle scanning phased array," *Int. J. RF Microwave Computer-Aided Eng.*, vol. 31, no. 9, Sep. 2021.

[15] J. Hu, Y. Li, and Z. Zhang, "Vertically polarized 360° azimuth scanning array," *IEEE Antennas Wirel. Propag. Lett.*, vol. 21, no. 5, pp. 898–902, May 2022.

[16] S. Gishkori, D. Wright, L. Daniel, A. Shaikh, T. Al-Naffouri, M. Gashinova, and B. Mulgrew, "Adaptive subaperture integration for wide-angle synthetic aperture radar," *IEEE Trans. Terahertz Sci. Technol.*, vol. 12, no. 2, pp. 118–129, 2021.

[17] L. B. S. Kavitha and I. J. Raglend, "A wide-scan phased array antenna for a small active electronically scanned array: A review," in *2013 International Conference on Circuits, Power and Computing Technologies (ICCPCT)*. IEEE, 2013, pp. 1008–1016.

[18] Y. Li, S. Xiao, and J. Guo, "A review of wideband wide-angle scanning 2-D phased array and its applications in satellite com-

munication," *Journal of Communications and Information Networks*, vol. 3, no. 1, pp. 21–30, Mar. 2018.

[19] S. Gao, Y. J. Guo, S. A. Safavi-Naeini, W. Hong, and X.-X. Yang, "Guest editorial low-cost wide-angle beam-scanning antennas," *IEEE Trans. Antennas Propag.*, vol. 70, no. 9, pp. 7378–7383, Sep. 2022.

[20] Y. Liu, J. Zheng, M. Li, Q. Luo, Y. Rui, and Y. Guo, "Synthesizing beam-scannable thinned massive antenna array utilizing modified iterative FFT for millimeter-wave communication," *IEEE Antennas Wirel. Propag. Lett.*, vol. 19, no. 11, 2020.

[21] K. Yang, Z. Zhao, and Q. H. Liu, "Fast pencil beam pattern synthesis of large unequally spaced antenna arrays," *IEEE Trans. Antennas Propag.*, vol. 61, no. 2, pp. 627–634, Feb. 2012.

[22] Y. Liu, L. Chen, C. Zhu, Y.-L. Ban, and Y. J. Guo, "Efficient and accurate frequency-invariant beam pattern synthesis utilizing iterative spatiotemporal Fourier transform," *IEEE Trans. Antennas Propag.*, vol. 68, no. 8, pp. 6069–6079, Aug. 2020.

[23] Y. Liu, Y. Yang, P. Wu, X. Ma, M. Li, K.-D. Xu, and Y. J. Guo, "Synthesis of multibeam sparse circular-arc antenna arrays employing refined extended alternating convex optimization," *IEEE Trans. Antennas Propag.*, vol. 69, no. 1, pp. 566–571, Jan. 2020.

[24] P. You, Y. Liu, S.-L. Chen, K. Da Xu, W. Li, and Q. H. Liu, "Synthesis of unequally spaced linear antenna arrays with minimum element spacing constraint by alternating convex optimization," *IEEE Antennas Wirel. Propag. Lett.*, vol. 16, pp. 3126–3130, 2017.

[25] J. L. A. Quijano and G. Vecchi, "Alternating adaptive projections in antenna synthesis," *IEEE Trans. Antennas Propag.*, vol. 58, no. 3, pp. 727–737, Mar. 2009.

[26] Y. Han, C. Wan, W. Sheng, B. Tian, and H. Yang, "Array synthesis using weighted alternating projection and proximal splitting," *IEEE Antennas Wirel. Propag. Lett.*, vol. 14, pp. 1006–1009, 2015.

[27] Y. Ma, S. Yang, Y. Chen, S.-W. Qu, and J. Hu, "Pattern synthesis of 4-D irregular antenna arrays based on maximum-entropy model," *IEEE Trans. Antennas Propag.*, vol. 67, no. 5, pp. 3048–3057, May 2019.

[28] R. Li, L. Xu, X.-W. Shi, N. Zhang, and Z.-Q. Lv, "Improved differential evolution strategy for antenna array pattern synthesis problems," *Prog. Electromagn. Res.*, vol. 113, pp. 429–441, 2011.

[29] Q. Wu, W. Chen, C. Yu, H. Wang, and W. Hong, "Knowledge-guided active-base-element modeling in machine-learning-assisted antenna-array design," *IEEE Trans. Antennas Propag.*, vol. 71, no. 2, pp. 1578–1589, Feb. 2023.

[30] C. Cui, W. T. Li, X. T. Ye, Y. Q. Hei, P. Rocca, and X. W. Shi, "Synthesis of mask-constrained pattern-reconfigurable nonuniformly spaced linear arrays using artificial neural networks," *IEEE Trans. Antennas Propag.*, vol. 70, no. 6, pp. 4355–4368, Jun. 2022.

[31] B. Zhang, C. Jin, K. Cao, Q. Lv, and R. Mittra, "Cognitive conformal antenna array exploiting deep reinforcement learning method," *IEEE Trans. Antennas Propag.*, vol. 70, no. 7, pp. 5094–5104, Jul. 2022.

[32] A. Trastoy, F. Ares, and E. Moreno, "Phase-only control of antenna sum and shaped patterns through null perturbation," *IEEE Antennas Propag. Mag.*, vol. 43, no. 6, pp. 45–54, Dec. 2001.

[33] D. P. Scholnik, "A parameterized pattern-error objective for large-scale phase-only array pattern design," *IEEE Trans. Antennas Propag.*, vol. 64, no. 1, pp. 89–98, Jan. 2015.

[34] T. Van Luyen and T. Vu Bang Giang, "Interference suppression of ULA antennas by phase-only control using bat algorithm," *IEEE Antennas Wirel. Propag. Lett.*, vol. 16, pp. 3038–3042, 2017.

[35] J. Liang, X. Fan, W. Fan, D. Zhou, and J. Li, "Phase-only pattern synthesis for linear antenna arrays," *IEEE Antennas Wirel. Propag. Lett.*, vol. 16, pp. 3232–3235, 2017.

[36] R. L. Haupt and D. W. Aten, "Low sidelobe arrays via dipole rotation," *IEEE Trans. Antennas Propag.*, vol. 57, no. 5, pp. 1575–1579, May 2009.

[37] J. I. Echeveste, J. Rubio, M. Á. G. de Aza, and C. Craeye, "Pattern synthesis of coupled antenna arrays via element rotation," *IEEE Antennas Wirel. Propag. Lett.*, vol. 16, pp. 1707–1710, 2017.

[38] A. Smolders and H. Visser, "Low side-lobe circularly-polarized phased arrays using a random sequential rotation technique," *IEEE Trans. Antennas Propag.*, vol. 62, no. 12, pp. 6476–6481, Dec. 2014.

[39] A. B. Smolders and U. Johannsen, "Axial ratio enhancement for circularly-polarized millimeter-wave phased-arrays using a sequential rotation technique," *IEEE Trans. Antennas Propag.*, vol. 59, no. 9, pp. 3465–3469, Sep. 2011.

[40] Y. Peng, Y. Liu, M. Li, H. Liu, and Y. J. Guo, "Synthesizing circularly polarized multi-beam planar dipole arrays with sidelobe and cross-polarization control by two-step element rotation and phase optimization," *IEEE Trans. Antennas Propag.*, vol. 70, no. 6, pp. 4379–4391, Jun. 2022.

[41] M. Li, Y. Liu, and Y. J. Guo, "Design of sum and difference patterns by optimizing element rotations and positions for linear dipole array," *IEEE Trans. Antennas Propag.*, vol. 69, no. 5, pp. 3027–3032, May 2021.

[42] M. Li, Y. Liu, and Y. Guo, "Shaped power pattern synthesis of a linear dipole array by element rotation and phase optimization using dynamic differential evolution," *IEEE Antennas Wirel. Propag. Lett.*, vol. 17, no. 4, 2018.

[43] Y. Liu, M. Li, R. L. Haupt, and Y. J. Guo, "Synthesizing shaped power patterns for linear and planar antenna arrays including mutual coupling by refined joint rotation/phase optimization," *IEEE Trans. Antennas Propag.*, vol. 68, no. 6, pp. 4648–4657, Jun. 2020.

[44] M. Li, Y. Liu, S.-L. Chen, J. Hu, and Y. J. Guo, "Synthesizing shaped-beam cylindrical conformal array considering mutual coupling using refined rotation/phase optimization," *IEEE Trans. Antennas Propag.*, vol. 70, no. 11, pp. 10543–10553, Nov. 2022.

[45] R. C. Hansen, *Phased array antennas*. John Wiley & Sons, 2009.

[46] R. J. Mailloux, *Phased Array Antenna Handbook*, 2nd ed., ser. Artech House Antennas and Propagation Library, Boston, 2005.

[47] S. Liu, K. Jiang, G. Xu, X. Ding, K. Zhang, J. Fu, and Q. Wu, "A dual-band shared aperture antenna array in Ku/Ka-bands for beam scanning applications," *IEEE Access*, vol. 7, pp. 78794–78802, 2019.

[48] Y. F. Cheng, X. Ding, G. F. Gao, W. Shao, and C. Liao, "Analysis and design of wide-scan phased array using polarization-conversion isolators," *IEEE Antennas Wirel. Propag. Lett.*, vol. 18, no. 3, pp. 512–516, Mar. 2019.

[49] R. Wang, B. Z. Wang, X. Ding, and X. S. Yang, "Planar phased array with wide-angle scanning performance based on image theory," *IEEE Trans. Antennas Propag.*, vol. 63, no. 9, pp. 3908–3917, Sep. 2015.

[50] Y. F. Cheng, J. Feng, C. Liao, and X. Ding, "Analysis and design of wideband low-RCS wide-scan phased array with AMC ground," *IEEE Antennas Wirel. Propag. Lett.*, vol. 20, no. 2, pp. 209–213, Feb. 2021.

[51] Y. Q. Wen, B. Z. Wang, and X. Ding, "A wide-angle scanning and low sidelobe level microstrip phased array based on genetic algorithm optimization," *IEEE Trans. Antennas Propag.*, vol. 64, no. 2, pp. 805–810, Feb. 2016.

[52] ——, "Wide-beam SIW-slot antenna for wide-angle scanning phased array," *IEEE Antennas Wirel. Propag. Lett.*, vol. 15, pp. 1638–1641, 2016.

[53] Y. F. Cheng, X. Ding, W. Shao, and C. Liao, "A high-gain sparse phased array with wide-angle scanning performance and low sidelobe levels," *IEEE Access*, vol. 7, pp. 31151–31158, 2019.

[54] B. F. Sun, X. Ding, Y. F. Cheng, and W. Shao, "Substrate integrated waveguide-slot wide-angle scanning aperiodic phased array with low side-lobe levels," *Microw Opt. Technol. Lett.*, vol. 62, no. 1, pp. 210–216, Jan. 2020.

[55] C. M. Liu, S. Q. Xiao, H. L. Tu, and Z. Ding, "Wide-angle scanning low profile phased array antenna based on a novel magnetic dipole," *IEEE Trans. Antennas Propag.*, vol. 65, no. 3, pp. 1151–1162, Mar. 2017.

[56] C. M. Liu, S. Xiao, and X. L. Zhang, "A compact, low-profile wire antenna applied to wide-angle scanning phased array," *IEEE Antennas Wirel. Propag. Lett.*, vol. 17, no. 3, pp. 389–392, Mar. 2018.

[57] G. Yang, J. Li, D. Wei, and R. Xu, "Study on wide-angle scanning linear phased array antenna," *IEEE Trans. Antennas Propag.*, vol. 66, no. 1, pp. 450–455, Jan. 2018.

[58] G. W. Yang and S. Zhang, "A dual-band shared-aperture antenna with wide-angle scanning capability for mobile system applications," *IEEE Trans. Veh. Technol.*, vol. 70, no. 5, pp. 4088–4097, May 2021.

[59] G. Yang, J. Li, S. G. Zhou, and Y. Qi, "A wide-angle E-plane scanning linear array antenna with wide beam elements," *IEEE Antennas Wirel. Propag. Lett.*, vol. 16, pp. 2923–2926, Sep. 2017.

[60] Q. Zhang, W. Jiang, P. Liu, K. Wei, W. Hu, and S. Gong, "Metamaterial-based linear phased array antenna with improved wide-angle scanning bandwidth by parasitic metal strips," *IET Microw., Antennas and Propag.*, vol. 15, no. 13, pp. 1699–1709, Oct. 2021.

[61] L. X. Guan, Y. F. Cheng, J. Feng, and C. Liao, "A novel planar wide-angle scanning phased array under operation of TM_{10} and TM_{20} modes," *Microw Opt. Technol. Lett.*, vol. 63, no. 3, pp. 944–951, Mar. 2021.

[62] B. F. Sun, X. Ding, Y. F. Cheng, and W. Shao, "2-D wide-angle scanning phased array with hybrid patch mode technique," *IEEE Antennas Wirel. Propag. Lett.*, vol. 19, no. 4, pp. 700–704, Apr. 2020.

[63] Y. Q. Wen, S. Gao, B. Z. Wang, and Q. Luo, "Dual-polarized and wide-angle scanning microstrip phased array," *IEEE Trans. Antennas Propag.*, vol. 66, no. 7, pp. 3775–3780, Jul. 2018.

[64] C. Y. Wei, H. C. Zhang, P. H. He, L. P. Zhang, X. T. Yan, J. Lu, and T. J. Cui, "A dual circularly polarized SIW-fed phased array antenna with wide-angle beam scanning range," *IEEE Trans. Antennas Propag.*, vol. 70, no. 9, pp. 7393–7402, Sep. 2022.

[65] Y. F. Cheng, X. Ding, W. Shao, M. X. Yu, and B. Z. Wang, "2-D planar wide-angle scanning-phased array based on wide-beam elements," *IEEE Antennas Wirel. Propag. Lett.*, vol. 16, pp. 876–879, 2017.

[66] Y. Q. Wen, B. Z. Wang, and X. Ding, "Wide-beam circularly polarized microstrip magnetic-electric dipole antenna for wide-angle scanning phased array," *IEEE Antennas Wirel. Propag. Lett.*, vol. 16, pp. 428–431, 2017.

[67] Z. Wang, S. Zhao, and Y. Dong, "Metamaterial-based wide-beam dielectric resonator antenna for broadband wide-angle beam-scanning phased array applications," *IEEE Trans. Antennas Propag.*, vol. 70, no. 10, pp. 9061–9072, Oct. 2022.

[68] Z.-L. Su, K. W. Leung, and K. Lu, "A shaped-beam antenna for wide-angle scanning phased array," *IEEE Trans. Antennas Propag.*, vol. 70, no. 9, pp. 7659–7669, Sep. 2022.

[69] S. H. Zhu, X. S. Yang, L. L. Wang, and J. Wang, "Hybrid topology optimization of dual-polarized wide-beam antenna and its application in wide-angle scanning array," *Int. J. RF Microwave Computer-Aided Eng.*, vol. 32, no. 3, Mar. 2022.

[70] Y.-F. Cheng, Z.-H. Gao, L. Yang, and C. Liao, "A planar end-loaded dipole phased array with enhanced bandwidth and wide-angle scan," *Int. J. RF Microwave Computer-Aided Eng.*, vol. 31, no. 10, Oct. 2021.

[71] G. Yang, J. Li, R. Xu, Y. Ma, and Y. Qi, "Improving the performance of wide-angle scanning array antenna with a high-impedance periodic structure," *IEEE Antennas Wirel. Propag. Lett.*, vol. 15, pp. 1819–1822, 2016.

[72] M. Li, S. Q. Xiao, and B. Z. Wang, "Investigation of using high impedance surfaces for wide-angle scanning arrays," *IEEE Trans. Antennas Propag.*, vol. 63, no. 7, pp. 2895–2901, Jul. 2015.

[73] X. Ding, Y. F. Cheng, W. Shao, and B. Z. Wang, "A wide-angle scanning phased array with microstrip patch mode reconfiguration technique," *IEEE Trans. Antennas Propag.*, vol. 65, no. 9, pp. 4548–4555, Sep. 2017.

[74] G. F. Gao, X. Ding, Y. F. Cheng, and W. Shao, "Dual-polarized wide-angle scanning phased array based on mutimode patch elements," *IEEE Antennas Wirel. Propag. Lett.*, vol. 18, no. 3, pp. 546–550, Mar. 2019.

[75] Y. F. Cheng, X. Ding, W. Shao, and B. Z. Wang, "Planar wide-angle scanning phased array with pattern-reconfigurable windmill-shaped loop elements," *IEEE Trans. Antennas Propag.*, vol. 65, no. 2, pp. 932–936, Feb. 2017.

[76] Z. Chen, Z. Song, H. Liu, X. Liu, J. Yu, and X. Chen, "A compact phase-controlled pattern-reconfigurable dielectric resonator antenna for passive wide-angle beam scanning," *IEEE Trans. Antennas Propag.*, vol. 69, no. 5, pp. 2981–2986, May 2021.

[77] K. Wang, J. Geng, H. Zhou, S. Yang, R. Zhao, J. Chen, J. Lu, X. Tang, J. Zhang, and R. Jin, "A novel low-profile phased antenna with dual-port and its application in 1-D linear array to 2-D scanning," *IEEE Trans. Antennas Propag.*, vol. 70, no. 8, pp. 6718–6731, Aug. 2022.

[78] Z. Wang, S. Zhao, and Y. Dong, "Miniaturized, vertically polarized, pattern reconfigurable dielectric resonator antenna and its phased array for wide-angle beam steering," *IEEE Trans. Antennas Propag.*, vol. 70, no. 10, pp. 9233–9246, Oct. 2022.

[79] Y. F. Cheng, X. Ding, W. Shao, M. X. Yu, and B. Z. Wang, "A novel wide-angle scanning phased array based on dual-mode pattern-reconfigurable elements," *IEEE Antennas Wirel. Propag. Lett.*, vol. 16, pp. 396–399, 2017.

[80] A. Pal, A. Mehta, D. Mirshekar-Syahkal, and H. Nakano, "2 × 2 phased array consisting of square loop antennas for high gain wide angle scanning with low grating lobes," *IEEE Trans. Antennas Propag.*, vol. 65, no. 2, pp. 576–583, Feb. 2017.

[81] Z. Ding, J. Chen, H. Zhou, and R. Jin, "Two-dimensional scanning phased array with large element spacing using pattern reconfigurable stacked patch antenna at Ka-band," *IEEE Trans. Antennas Propag.*, vol. 70, no. 7, pp. 5447–5457, Jul. 2022.

[82] Y. Y. Bai, S. Xiao, M. C. Tang, Z. F. Ding, and B. Z. Wang, "Wide-angle scanning phased array with pattern reconfigurable elements," *IEEE Trans. Antennas Propag.*, vol. 59, no. 11, pp. 4071–4076, Nov. 2011.

[83] Y. Du, J. Y. Li, D. Li, L. K. Zhang, and W. J. Shu, "A linear wide-angle scanning phased array based on pattern reconfigurable elements," *Microw Opt. Technol. Lett.*, vol. 64, no. 5, pp. 926–932, May 2022.

[84] X. Ding, B.-Z. Wang, and G.-Q. He, "Research on a millimeter-wave phased array with wide-angle scanning performance," *IEEE Trans. Antennas Propag.*, vol. 61, no. 10, pp. 5319–5324, Oct. 2013.

[85] S. Xiao, C. Zheng, M. Li, J. Xiong, and B.-Z. Wang, "Varactor-loaded pattern reconfigurable array for wide-angle scanning with low gain fluctuation," *IEEE Trans. Antennas Propag.*, vol. 63, no. 5, pp. 2364–2369, May 2015.

[86] X. Chen, M. Abdullah, Q. Li, J. Li, A. Zhang, and T. Svensson, "Characterizations of mutual coupling effects on switch-based phased array antennas for 5G millimeter-wave mobile communications," *IEEE Access*, vol. 7, pp. 31376–31384, 2019.

[87] J. Yun, D. Park, D. Jang, and K. C. Hwang, "Design of an active beam-steering array with a perforated wide-angle impedance matching layer," *IEEE Trans. Antennas Propag.*, vol. 69, no. 9, pp. 6028–6033, Sep. 2021.

[88] T. R. Cameron and G. V. Eleftheriades, "Analysis and characterization of a wide-angle impedance matching metasurface for dipole phased arrays," *IEEE Trans. Antennas Propag.*, vol. 63, no. 9, pp. 3928–3938, Sep. 2015.

[89] D. Bianchi, S. Genovesi, M. Borgese, F. Costa, and A. Monorchio, "Element-independent design of wide-angle impedance matching radomes by using the generalized scattering matrix approach," *IEEE Trans. Antennas Propag.*, vol. 66, no. 9, pp. 4708–4718, Sep. 2018.

[90] S. Xiao, S. Yang, H. Zhang, Q. Xiao, Y. Chen, and S. W. Qu, "Practical implementation of wideband and wide-scanning cylindrically conformal phased array," *IEEE Trans. Antennas Propag.*, vol. 67, no. 8, pp. 5729–5733, Aug. 2019.

[91] B. Wang, X. Q. Lin, L. Y. Nie, and D. Q. Yu, "A broadband wide-scanning planar phased array antenna with equivalent circuit analysis," *IEEE Antennas Wirel. Propag. Lett.*, vol. 19, no. 12, pp. 2154–2158, Dec. 2020.

[92] J. A. Kasemodel, C. C. Chen, and J. L. Volakis, "Wideband planar array with integrated feed and matching network for wide-angle scanning," *IEEE Trans. Antennas Propag.*, vol. 61, no. 9, pp. 4528–4537, Sep. 2013.

[93] Y. Jia, J. Hu, Y. Liu, and Z. X. Liu, "A linear tightly coupled dipole array with wide-angle scanning," *Int. J. RF Microwave Computer-Aided Eng.*, vol. 32, no. 9, Sep. 2022.

[94] J. P. Doane, K. Sertel, and J. L. Volakis, "A wideband, wide scanning tightly coupled dipole array with integrated balun (TCDA-IB)," *IEEE Trans. Antennas Propag.*, vol. 61, no. 9, pp. 4538–4548, Sep. 2013.

[95] W. F. Moulder, K. Sertel, and J. L. Volakis, "Ultrawideband superstrate-enhanced substrate-loaded array with integrated feed," *IEEE Trans. Antennas Propag.*, vol. 61, no. 11, pp. 5802–5807, Nov. 2013.

[96] B. Wang, S. Yang, Y. Chen, S. Qu, and J. Hu, "Low cross-polarization ultrawideband tightly coupled balanced antipodal dipole array," *IEEE Trans. Antennas Propag.*, vol. 68, no. 6, pp. 4479–4488, Jun. 2020.

[97] S. Hussain, S. W. Qu, W. L. Zhou, P. Zhang, and S. Yang, "Design and fabrication of wideband dual-polarized dipole array for 5G wireless systems," *IEEE Access*, vol. 8, pp. 65155–65163, 2020.

[98] S. Hussain, S. W. Qu, P. Zhang, X. H. Wang, and S. Yang, "A low-profile, wide-scan, cylindrically conformal X-band phased array," *IEEE Antennas Wirel. Propag. Lett.*, vol. 20, no. 8, pp. 1503–1507, Aug. 2021.

[99] B. Wang, S. Yang, Z. Zhang, Y. Chen, S. Qu, and J. Hu, "A ferrite-loaded ultralow profile ultrawideband tightly coupled dipole array," *IEEE Trans. Antennas Propag.*, vol. 70, no. 3, pp. 1965–1975, Mar. 2022.

[100] A. O. Bah, P. Y. Qin, R. W. Ziolkowski, Y. J. Guo, and T. S. Bird, "A wideband low-profile tightly coupled antenna array with a very high figure of merit," *IEEE Trans. Antennas Propag.*, vol. 67, no. 4, pp. 2332–2343, Apr. 2019.

[101] J. X. Sun, Y. J. Cheng, Y. F. Wu, and Y. Fan, "Ultrawideband, low-profile, and low-RCS conformal phased array with capacitance-integrated balun and multifunctional meta-surface," *IEEE Trans. Antennas Propag.*, vol. 70, no. 9, pp. 7448–7457, Sep. 2022.

[102] H. Zhang, S. Yang, Y. Chen, J. Guo, and Z. Nie, "Wideband dual-polarized linear array of tightly coupled elements," *IEEE Trans. Antennas Propag.*, vol. 66, no. 1, pp. 476–480, Jan. 2018.

[103] J. Zhong, A. Johnson, E. A. Alwan, and J. L. Volakis, "Dual-linear polarized phased array with 9:1 bandwidth and 60° scanning off broadside," *IEEE Trans. Antennas Propag.*, vol. 67, no. 3, pp. 1996–2001, Mar. 2019.

[104] Z. Jiang, S. Xiao, and B.-Z. Wang, "A low-cost light-weight ultrawideband wide-angle scanning tightly coupled dipole array loaded with multilayer metallic strips," *IEEE Access*, vol. 9, pp. 24 975–24 983, 2021.

[105] H. Zhang, S. Yang, S. W. Xiao, Y. Chen, S. W. Qu, and J. Hu, "Ultrawideband phased antenna arrays based on tightly coupled open folded dipoles," *IEEE Antennas Wirel. Propag. Lett.*, vol. 18, no. 2, pp. 378–382, Feb. 2019.

[106] E. Yetisir, N. Ghalichechian, and J. L. Volakis, "Ultrawideband array with 70° scanning using FSS superstrate," *IEEE Trans. Antennas Propag.*, vol. 64, no. 10, pp. 4256–4265, Oct. 2016.

[107] C. H. Hu, B. Z. Wang, R. Wang, S. Q. Xiao, and X. Ding, "Ultrawideband, wide-angle scanning array with compact, single-layer feeding network," *IEEE Trans. Antennas Propag.*, vol. 68, no. 4, pp. 2788–2796, Apr. 2020.

[108] Y. Rahmat-Samii, "Electromagnetic band-gap structures: Classification, characterization, and applications," in *11th International Conference on Antennas and Propagation (ICAP 2001)*, vol. 2001, 2001, pp. 560–564.

[109] F. Yang and Y. Rahmat-Samii, "Microstrip antennas integrated with electromagnetic band-gap (EBG) structures: A low mutual coupling design for array applications," *IEEE Trans. Antennas Propag.*, vol. 51, no. 10, pp. 2936–2946, Oct. 2003.

[110] W. M. Zou, S. W. Qu, and S. Yang, "Wideband wide-scanning phased array in triangular lattice with electromagnetic bandgap structures," *IEEE Antennas Wirel. Propag. Lett.*, vol. 18, no. 3, pp. 422–426, Mar. 2019.

[111] K. Wei, J.-Y. Li, L. Wang, Z.-J. Xing, and R. Xu, "Mutual coupling reduction by novel fractal defected ground structure bandgap filter," *IEEE Trans. Antennas Propag.*, vol. 64, no. 10, pp. 4328–4335, Oct. 2016.

[112] L. Gu, Y. W. Zhao, Q. M. Cai, Z. P. Zhang, B. H. Xu, and Z. P. Nie, "Scanning enhanced low-profile broadband phased array with radiator-sharing approach and defected ground structures," *IEEE Trans. Antennas Propag.*, vol. 65, no. 11, pp. 5846–5854, Nov. 2017.

[113] Y. Li and S. Xiao, "Wideband wide-angle scanning phased array based on miniaturized metasurface antenna," *IEEE Trans. Antennas Propag.*, vol. 70, no. 2, pp. 1107–1119, Feb. 2022.

[114] K. L. Wu, C. Wei, X. Mei, and Z. Y. Zhang, "Array-antenna decoupling surface," *IEEE Trans. Antennas Propag.*, vol. 65, no. 12, pp. 6728–6738, Dec. 2017.

[115] B. Xi, Y. Xiao, M. Li, Y. Li, H. Sun, and Z. Chen, "Wide-angle scanning phased array antennas using metasurface slabs," *IEEE Trans. Antennas Propag.*, vol. 69, no. 12, pp. 9003–9008, Dec. 2021.

[116] B. Yan, L. Sun, W. Sheng, and Z. N. Chen, "Reactive impedance surface-loaded wideband wide-scanning phased array in triangular lattice," *IEEE Trans. Antennas Propag.*, vol. 70, no. 5, pp. 3366–3373, May 2022.

[117] X. Ding, Y. F. Cheng, W. Shao, and B. Z. Wang, "Broadband low-RCS phased array with wide-angle scanning performance based on the switchable stacked artificial structure," *IEEE Trans. Antennas Propag.*, vol. 67, no. 10, pp. 6452–6460, Oct. 2019.

[118] A. Vosoogh and P.-S. Kildal, "Simple formula for aperture efficiency reduction due to grating lobes in planar phased arrays," *IEEE Trans. Antennas Propag.*, vol. 64, no. 6, pp. 2263–2269, Jun. 2016.

[119] B. A. Arand, A. Bazrkar, and A. Zahedi, "Design of a phased array in triangular grid with an efficient matching network and reduced mutual coupling for wide-angle scanning," *IEEE Trans. Antennas Propag.*, vol. 65, no. 6, pp. 2983–2991, Jun. 2017.

[120] X. Zhang, S. Xiao, C. Liu, Z. Wang, J. Deng, and X. Bai, "A wideband and circularly polarized wide-angle scanning phased array with substrate-integrated cavity-backed patches," Tech. Rep., 2018.

[121] R. W. Kindt and B. T. Binder, "Wideband, low-profile, dual-polarized machined-metal array on a triangular lattice," *IEEE Trans. Antennas Propag.*, vol. 70, no. 2, pp. 1097–1106, Feb. 2022.

[122] H. Wang, D.-G. Fang, and Y. L. Chow, "Grating lobe reduction in a phased array of limited scanning," *IEEE Trans. Antennas Propag.*, vol. 56, no. 6, pp. 1581–1586, Jun. 2008.

[123] M. Bray, D. Werner, D. Boeringer, and D. Machuga, "Optimization of thinned aperiodic linear phased arrays using genetic algorithms to reduce grating lobes during scanning," *IEEE Trans. Antennas Propag.*, vol. 50, no. 12, pp. 1732–1742, Dec. 2002.

[124] P. Gu, Z. He, J. Xu, K. W. Leung, and R. S. Chen, "Design of wide scanning sparse planar array using both matrix-pencil and space-mapping methods," *IEEE Antennas Wirel. Propag. Lett.*, vol. 20, no. 2, pp. 140–144, Feb. 2021.

[125] A. Kedar, "Deterministic synthesis approach for linear sparse array antennas," *IEEE Trans. Antennas Propag.*, vol. 68, no. 9, pp. 6667–6674, Sep. 2020.

[126] X. Xu, C. Liao, L. Zhou, and F. Peng, "Grating lobe suppression of non-uniform arrays based on position gradient and sigmoid function," *IEEE Access*, vol. 7, pp. 106 407–106 416, 2019.

[127] Z. Iqbal and M. Pour, "Grating lobe reduction in scanning phased array antennas with large element spacing," *IEEE Trans. Antennas Propag.*, vol. 66, no. 12, pp. 6965–6974, Dec. 2018.

[128] ——, "Exploiting higher order modes for grating lobe reduction in scanning phased array antennas," *IEEE Trans. Antennas Propag.*, vol. 67, no. 11, pp. 7144–7149, Nov. 2019.

[129] Q. Ren, B. Qian, X. Chen, X. Huang, Q. Li, J. Zhang, and A. A. Kishk, "Linear antenna array with large element spacing for wide-angle beam scanning with suppressed grating lobes," *IEEE Antennas Wirel. Propag. Lett.*, vol. 21, no. 6, pp. 1258–1262, Jun. 2022.

[130] Z. DIng, J. Chen, H. Liu, C. He, and R. Jin, "Grating lobe suppression of sparse phased array by null scanning antenna," *IEEE Trans. Antennas Propag.*, vol. 70, no. 1, pp. 317–329, Jan. 2022.

[131] D. K. Karmokar, Y. J. Guo, P. Y. Qin, S. L. Chen, and T. S. Bird, "Substrate integrated waveguide-based periodic backward-to-forward scanning leaky-wave antenna with low cross-polarization," *IEEE Trans. Antennas Propag.*, vol. 66, no. 8, pp. 3846–3856, Aug. 2018.

[132] Z. Li, W. Cui, R. Liu, K. Zhang, W. Liang, M. Wang, C. Fan, H. Zheng, and E. Li, "Investigation of leaky-wave antenna with stable wide beam-scanning characteristic," *IEEE Trans. Antennas Propag.*, vol. 70, no. 1, pp. 240–249, Jan. 2022.

[133] D. R. Jackson, C. Caloz, and T. Itoh, "Leaky-wave antennas," in *Proceedings of the IEEE*, vol. 100, 2012, pp. 2194–2206.

[134] M. A. Antoniades and G. V. Eleftheriades, "A CPS leaky-wave antenna with reduced beam squinting using NRI-TL metamaterials," *IEEE Trans. Antennas Propag.*, vol. 56, no. 3, pp. 708–721, Mar. 2008.

[135] D.-F. Guan, Q. Zhang, P. You, Z.-B. Yang, Y. Zhou, and S.-W. Yong, "Scanning rate enhancement of leaky-wave antennas using slow-wave substrate integrated waveguide structure," *IEEE Trans. Antennas Propag.*, vol. 66, no. 7, pp. 3747–3751, Jul. 2018.

[136] D. K. Karmokar, S. L. Chen, D. Thalakotuna, P. Y. Qin, T. S. Bird, and Y. J. Guo, "Continuous backward-to-forward scanning 1-D slot-array leaky-wave antenna with improved gain," *IEEE Antennas Wirel. Propag. Lett.*, vol. 19, no. 1, pp. 89–93, Jan. 2020.

[137] S. L. Chen, D. K. Karmokar, Z. Li, P. Y. Qin, R. W. Ziolkowski, and Y. J. Guo, "Circular-polarized substrate-integrated-waveguide leaky-wave antenna with wide-angle and consistent-gain continuous beam scanning," *IEEE Trans. Antennas Propag.*, vol. 67, no. 7, pp. 4418–4428, Jul. 2019.

[138] D. K. Karmokar, S. L. Chen, T. S. Bird, and Y. J. Guo, "Single-layer multi-via loaded CRLH leaky-wave antennas for wide-angle beam scanning with consistent gain," *IEEE Antennas Wirel. Propag. Lett.*, vol. 18, no. 2, pp. 313–317, Feb. 2019.

[139] A. Mehdipour and G. V. Eleftheriades, "Leaky-wave antennas using negative-refractive-index transmission-line metamaterial supercells," *IEEE Trans. Antennas Propag.*, vol. 62, no. 8, pp. 3929–3942, Aug. 2014.

[140] D. K. Karmokar, Y. J. Guo, S. L. Chen, and T. S. Bird, "Composite right/left-handed leaky-wave antennas for wide-angle beam scan-

ning with flexibly chosen frequency range," *IEEE Trans. Antennas Propag.*, vol. 68, no. 1, pp. 100–110, Jan. 2020.

[141] S. L. Chen, D. K. Karmokar, Z. Li, P. Y. Qin, R. W. Ziolkowski, and Y. Jay Guo, "Continuous beam scanning at a fixed frequency with a composite right-/left-handed leaky-wave antenna operating over a wide frequency band," *IEEE Trans. Antennas Propag.*, vol. 67, no. 12, pp. 7272–7284, Dec. 2019.

[142] P. F. Zhang, L. Zhu, and S. Sun, "Microstrip-line EH_1/EH_2-mode leaky-wave antennas with backward-to-forward scanning," *IEEE Antennas Wirel. Propag. Lett.*, vol. 19, no. 12, pp. 2363–2367, 2020.

[143] H. Jiang, K. Xu, Q. Zhang, Y. Yang, D. K. Karmokar, S. Chen, P. Zhao, G. Wang, and L. Peng, "Backward-to-forward wide-angle fast beam-scanning leaky-wave antenna with consistent gain," *IEEE Trans. Antennas Propag.*, vol. 69, no. 5, pp. 2987–2992, May 2021.

[144] Y.-L. Lyu, F.-Y. Meng, G.-H. Yang, P.-Y. Wang, Q. Wu, and K. Wu, "Periodic leaky-wave antenna based on complementary pair of radiation elements," *IEEE Trans. Antennas Propag.*, vol. 66, no. 9, pp. 4503–4515, Sep. 2018.

[145] G. Zhang, Q. Zhang, Y. Chen, and R. D. Murch, "High-scanning-rate and wide-angle leaky-wave antennas based on glide-symmetry goubau line," *IEEE Trans. Antennas Propag.*, vol. 68, no. 4, pp. 2531–2540, Apr. 2020.

[146] K. Rudramuni, K. Kandasamy, Q. Zhang, X.-L. Tang, A. Kandwal, P. K. T. Rajanna, and H. Liu, "Goubau-line leaky-wave antenna for wide-angle beam scanning from backfire to endfire," *IEEE Antennas Wirel. Propag. Lett.*, vol. 17, no. 8, pp. 1571–1574, 2018.

[147] J. Y. Yin, J. Ren, Q. Zhang, H. C. Zhang, Y. Q. Liu, Y. B. Li, X. Wan, and T. J. Cui, "Frequency-controlled broad-angle beam scanning of patch array fed by spoof surface plasmon polaritons," *IEEE Trans. Antennas Propag.*, vol. 64, no. 12, pp. 5181–5189, Dec. 2016.

[148] H.-R. Zu, B. Wu, and T. Su, "Beam manipulation of antenna with large frequency-scanning angle based on field confinement of spoof surface plasmon polaritons," *IEEE Trans. Antennas Propag.*, vol. 70, no. 4, pp. 3022–3027, Apr. 2022.

[149] S.-D. Xu, D.-F. Guan, Q. Zhang, P. You, S. Ge, X.-X. Hou, Z.-B. Yang, and S.-W. Yong, "A wide-angle narrowband leaky-wave antenna based on substrate integrated waveguide-spoof surface plasmon polariton structure," *IEEE Antennas Wirel. Propag. Lett.*, vol. 18, no. 7, pp. 1386–1389, 2019.

[150] H. Wang, S. Sun, X. Xue, P. Zhang, and B. Xu, "A periodic coplanar strips leaky-wave antenna with horizontal wide-angle beam scanning and stable radiation," *IEEE Trans. Antennas Propag.*, vol. 70, no. 10, pp. 9861–9866, Oct. 2022.

[151] J. Xiao, S. Liao, Q. Xue, and W. Che, "Millimeter-wave 1-D wide-angle scanning pseudo-curved surface conformal phased array antennas based on elongated planar aperture element," *IEEE Trans. Antennas Propag.*, vol. 71, no. 4, pp. 3731–3735, Apr. 2023.

[152] S. M. Moghaddam, J. Yang, and A. U. Zaman, "Fully-planar ultra-wideband tightly-coupled array (FPU-TCA) with integrated feed for wide-scanning millimeter-wave applications," *IEEE Trans. Antennas Propag.*, vol. 68, no. 9, pp. 6591–6601, Sep. 2020.

[153] C. A. Guo and Y. J. Guo, "A general approach for synthesizing multibeam antenna arrays employing generalized joined coupler matrix," *IEEE Trans. Antennas Propag.*, vol. 70, no. 9, pp. 7556–7564, Sep. 2022.

[154] C. A. Guo, Y. J. Guo, H. Zhu, W. Ni, and J. Yuan, "Optimization of multibeam antennas employing generalized joined coupler matrix," *IEEE Trans. Antennas Propag.*, vol. 71, no. 1, pp. 215–224, Jan. 2023.

Ming Li was born in Anhui, China. He received the B.S. degree in electronic information science and technology and the M.S. degree in electromagnetic field and microwave technology from the Xiamen University (XMU), China, in 2015 and 2018, respectively, and the Ph.D. degree in Engineering from the Global Big Data Technologies Centre (GBTDC), University of Technology Sydney (UTS), Australia, in 2023. From May 2021 to July 2022, he was a Visiting Ph.D. Student with the Yangtze Delta Region Institute (Quzhou), University of Electronic Science and Technology of China (UESTC), Quzhou, China. Since February 2023, he has been a Research Assistant with the Global Big Data Technologies Centre (GBDTC), UTS. His current research interests include antenna array design and multibeam antennas.

Mr. Li was a recipient of the Honorable Mention at the IEEE International Symposium on Antennas and Propagation (AP-S), Denver 2022, the First Prize of Student Paper at the International Applied Computational Electromagnetics Society Symposium (ACES), Chengdu 2021, and the Student Representative Paper Award at the National Conference on Antennas (NCANT), Ningbo 2021.

Shu-Lin Chen (M'20) was born in Hubei Province, China. He received the B.S. degree in electrical engineering from Fuzhou University (FZU), China, in 2012; the M.S. degree in electromagnetic field and microwave technology from Xiamen University (XMU), China, in 2015; and the Ph.D. degree in engineering from the University of Technology Sydney (UTS), Australia, in 2019. From April to July 2019, he was a Research Associate with the State Key Laboratory of Terahertz and Millimeter Waves, City University of Hong Kong (CityU). From 2019 to 2022, he was a postdoctoral researcher with the Global Big Data Technologies Centre (GBDTC), UTS, where he is currently appointed as a Lecturer.

Dr Chen's research interests include reconfigurable antennas, leaky-wave antennas, and millimeter-wave and terahertz antennas. He received the Outstanding Master's Thesis of Fujian Province in 2015. He was a co-recipient for a number of prestigious conference paper awards, including the Honorable Mention Award in 2017 IEEE AP-S/URSI, the Best Paper Award Finalists in 2017 ISAP, the Best Paper Award in 2018 ISAPE, the First Prize of Student Paper in 2021 ACES, and the Best Young Professional Award in 2022 ISAP. He was awarded the TICRA-EurAAP Travel Grant for the 2022 EuCAP and the 2022 IEEE Antennas and Propagation Society (AP-S) Fellowship. He received the Outstanding Reviewer Awards (2020, 2021, and 2022) from the IEEE Antennas and Propagation Society.

Yanhui Liu (Senior Member, IEEE) received the B.S. and Ph.D. degrees in electrical engineering from the University of Electronic Science and Technology of China (UESTC), Chengdu, China, in 2004 and 2009, respectively.

From September 2007 to June 2009, he was a Visiting Scholar with the Department of Electrical and Computer Engineering, Duke University, Durham, NC, USA. In July 2011, he joined the Department of Electronic Science, Xiamen University, Xiamen, China, where he was, five years later, promoted to a Full Professor. From September to December 2017, he was a Visiting Professor with the State Key Laboratory of Millimeter Waves, City University of Hong Kong, Hong Kong. From December 2017 to December 2019, he was a Visiting Professor/Research Principal with the Global Big Data Technologies Centre, University of Technology Sydney (UTS), Ultimo, NSW, Australia. Since November 2019, he has been a Professor with UESTC. He has authored or coauthored over 120 peer-reviewed journal articles and 50 international conference papers. He holds 21 Chinese invention patents in antennas and applied electromagnetics. His research interests include antenna array design, reconfigurable antennas, and electromagnetic scattering and imaging.

Dr. Liu has served many times as a TPC member/reviewer/session chair in a number of international conferences in the field of antennas and propagation. He was a recipient of the UESTC Outstanding Graduate Award in 2004, the Outstanding Doctoral Dissertation Award of Sichuan Province of China in 2011, the Sichuan Province Distinguished Expert in 2021, and the Young Scientist Awards of PIERS in 2022. He is serving as a reviewer for a dozen of SCI-indexed journals. Since 2018, he has been serving as an Associate Editor for the IEEE ACCESS.
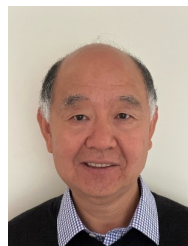
Y. Jay Guo (Fellow'2014) received a Bachelor's Degree and a Master's Degree from Xidian University in 1982 and 1984, respectively, and a Ph.D Degree from Xian Jiaotong University in 1987, all in China. His research interests include antennas, mm-wave and THz communications and sensing systems as well as big data technologies. He has published five books and over 700 research papers including over 300 IEEE Transactions papers, and he holds 26 international patents. His research interest includes multibeam antenna systems, reconfigurable antennas and metasurfaces, and joined communications and sensing for 6G.

Jay is a Fellow of the Australian Academy of Engineering and Technology and a Fellow of IEEE. He was a member of the College of Experts of Australian Research Council (ARC, 2016-2018). Jay has won a number of the most prestigious Australian national awards including the Engineering Excellence Awards (2007, 2012) and CSIRO Chairman's Medal (2007, 2012). He was named one of the most influential engineers in Australia in 2014 and 2015, and Australia's Research Field Leader in Electromagnetism by the Australian Research Report for three consecutive years since 2020. Together with his students and postdocs, he has won numerous best paper awards. In 2023, Jay received the prestigious IEEE APS Sergei A. Schelkunoff Transactions Paper Prize Award.

Jay is a Distinguished Professor and the Director of Global Big Data Technologies Centre (GBDTC) at the University of Technology Sydney (UTS), Australia. He is the founding Technical Director of the New South Wales (NSW) Connectivity Innovation Network (CIN). Prior to joining UTS in 2014, Jay served as a Director in CSIRO for over nine years. Before joining CSIRO, he held various senior technology leadership positions in Fujitsu, Siemens and NEC in the U.K.

Jay has chaired numerous international conferences and served as a guest editor for a number of IEEE publications. He was the Chair of International Steering Committee, International Symposium on Antennas and Propagation (2019-2021). He has been the International Advisory Committee Chair of IEEE VTC2017, General Chair of ISAP2022, ISAP2015, iWAT2014 and WPMC'2014, and TPC Chair of 2010 IEEE WCNC, and 2012 and 2007 IEEE ISCIT. He served as Guest Editor of special issues on "*Low-Cost Wide-Angle Beam Scanning Antennas*", "*Antennas for Satellite Communications*" and "*Antennas and Propagation Aspects of 60-90 GHz Wireless Communications*", all in IEEE Transactions on Antennas and Propagation, Special Issue on "*Communications Challenges and Dynamics for Unmanned Autonomous Vehicles*", IEEE Journal on Selected Areas in Communications (JSAC), and Special Issue on "*5G for Mission Critical Machine Communications*", IEEE Network Magazine.